

Structure Activity Relationships of 5-, 6-, and 7-Methyl-Substituted Azepan-3-one Cathepsin K Inhibitors

Dennis S. Yamashita,^{*,†} Robert W. Marquis,[†] Ren Xie,[†] Sirishkumar D. Nidamarthy,[†] Hye-Ja Oh,[†] Jae U. Jeong,[†] Karl F. Erhard,[†] Keith W. Ward,[‡] Theresa J. Roethke,[‡] Brian R. Smith,[‡] H-Y. Cheng,[§] Xiaoliu Geng,[§] Fan Lin,[§] Priscilla H. Offen,[§] Bing Wang,[§] Neysa Nevins,[§] Martha S. Head,[§] R. Curtis Haltiwanger,[§] Amy A. Narducci Sarjeant,[§] Louise M. Liable-Sands,[§] Baoguang Zhao,[§] Ward W. Smith,[§] Cheryl A. Janson,[§] Enoch Gao,^{||} Thaddeus Tomaszek,^{||} Michael McQueney,^{||} Ian E. James,[⊥] Catherine J. Gress,[⊥] Denise L. Zembryki,[⊥] Michael W. Lark,[⊥] and Daniel F. Veber[†]

Departments of Medicinal Chemistry; Drug Metabolism and Pharmacokinetics; Musculoskeletal Diseases Biology; Computational, Analytical, and Structural Sciences; and Screening and Compound Profiling, GlaxoSmithKline, 1250 S. Collegeville Rd, Collegeville, Pennsylvania 19426

Received September 14, 2005

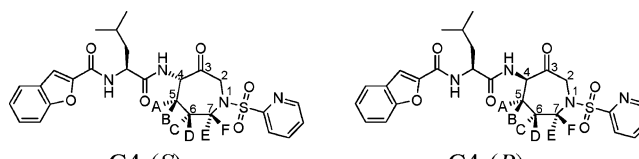
The syntheses, in vitro characterizations, and rat and monkey in vivo pharmacokinetic profiles of a series of 5-, 6-, and 7-methyl-substituted azepanone-based cathepsin K inhibitors are described. Depending on the particular regiochemical substitution and stereochemical configuration, methyl-substituted azepanones were identified that had widely varied cathepsin K inhibitory potency as well as pharmacokinetic properties compared to the 4*S*-parent azepanone analogue, **1** (human cathepsin K, $K_{i,app} = 0.16$ nM, rat oral bioavailability = 42%, rat in vivo clearance = 49.2 mL/min/kg). Of particular note, the 4*S*-7-*cis*-methylazepanone analogue, **10**, had a $K_{i,app} = 0.041$ nM vs human cathepsin K and 89% oral bioavailability and an in vivo clearance rate of 19.5 mL/min/kg in the rat. Hypotheses that rationalize some of the observed characteristics of these closely related analogues have been made using X-ray crystallography and conformational analysis. These examples demonstrate the potential for modulation of pharmacological properties of cathepsin inhibitors by substituting the azepanone core. The high potency for inhibition of cathepsin K coupled with the favorable rat and monkey pharmacokinetic characteristics of compound **10**, also known as SB-462795 or relacatib, has made it the subject of considerable in vivo evaluation for safety and efficacy as an inhibitor of excessive bone resorption in rat, monkey, and human studies, which will be reported elsewhere.

Introduction

Cathepsin K, a member of the papain-family of cysteine proteases, is highly expressed by osteoclasts and has been a therapeutic target of many drug discovery efforts aimed at identifying agents to treat disease states caused by excessive bone resorption such as osteoporosis.¹ In previously published papers, we have disclosed several classes of peptidomimetic ketone-based cathepsin K inhibitors² and have noted that by introducing an appropriate conformational constraint in the form of an azepan-3-one, cathepsin K inhibitory potency, rat oral bioavailability, and chemical stability could be improved.³ In this paper, we describe the effects of methyl-substitution of azepan-3-one analogues on cathepsin inhibitory potency and selectivity, chemical stability, cellular efficacy, and rat and monkey pharmacokinetic profiles.

As described in ref 3, an X-ray cocrystal structure of azepanone **1** (human cathepsin K $K_{i,app} = 0.16$ nM, Table 3; 42% rat oral bioavailability, Table 5) and human recombinant cathepsin K was determined. In this cocrystal structure, the amide group on the azepanone ring adopted an axial orientation on a chair conformer. This axial amide orientation was different from the one observed in the small molecule single-crystal X-ray diffraction study, where the amide group adopted an equatorial orientation on a different chair conformer (Figure 1 and Table 2). We were interested in identifying ways to further optimize

Table 1. Structures of Azepanone and Methyl-Substituted Azepanone Cathepsin Inhibitors



compd	C4	A	B	C	D	E	F
1	S	H	H	H	H	H	H
2	S	Me	H	H	H	H	H
3	S	H	Me	H	H	H	H
4	R	Me	H	H	H	H	H
5	R	H	Me	H	H	H	H
6	S	H	H	Me	H	H	H
7	S	H	H	H	Me	H	H
8	R	H	H	Me	H	H	H
9	R	H	H	H	Me	H	H
10	S	H	H	H	H	Me	H
11	S	H	H	H	H	H	Me
12	R	H	H	H	H	Me	H
13	R	H	H	H	H	H	Me

the inhibitory potency of azepanone **1** by lowering the activation barrier to access this bound chair conformer with an axial amide orientation. On the basis of the X-ray cocrystal structure of **1** bound to cathepsin K, we hypothesized that methyl substitution at the 5-, 6-, and 7- positions of the azepanone ring should be sterically tolerated by the enzyme. We also conjectured that methyl substitution of these positions should have considerable effects on ring conformations, rigidity, and chemical stability with respect to C4 epimerization and might also have an impact on pharmacokinetic properties such as oral bioavailability. Owing to the difficulties inherent in prediction of the impact

* To whom correspondence should be addressed. Tel.: (610) 917-7830. Fax: (610) 917-4206. Email: Dennis.S.Yamashita@gsk.com.

[†] Department of Medicinal Chemistry.

[‡] Department of Drug Metabolism and Pharmacokinetics.

[§] Department of Computational, Analytical, and Structural Sciences.

^{||} Department of Screening and Compound Profiling.

[⊥] Department of Musculoskeletal Diseases Biology.

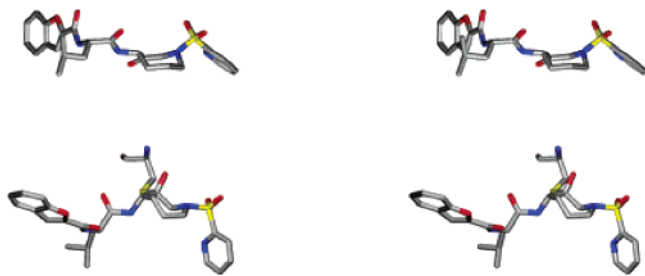


Figure 1. Stereoview comparison of single-molecule X-ray crystal structure of **1** (top) and human cathepsin K-1 cocrystal (bottom) structure conformations

of the methyl substitutions on preferred conformational preference, we synthesized and characterized all of the possible monomethyl-substituted azepanone analogues, **2–13**, shown in Table 1.

Synthesis of Methyl-Substituted Azepanones

Each position of methyl substitution on the azepanone ring as well as the diastereomeric forms of each of them presented unique challenges for chemical synthesis. Three basic chemical schemes were utilized to generate diastereomeric mixtures that were separated to give all of the possible forms for biological and biochemical characterization. Physical characterization of the individually isolated isomers as described below allowed exact definition of the geometric and stereochemical nature of each product.

An intramolecular nitroaldol (Henry) cyclization strategy⁴ was employed to synthesize the 5-methylazepanones (**2–5**), as shown in Scheme 1. Michael addition of nitromethane to ethyl crotonate (**14**) gave 3-methyl-4-nitrobutyrate (**15**). Reduction with DIBAL-H provided the aldehyde **16**, which was converted with *N*-benzylethanolamine in the presence of sodium triacetoxyborohydride to nitro alcohol **17**. Oxidation of **17** using DMSO and oxalyl chloride furnished aldehyde **18**. Treatment of the crude intermediate aldehyde **18** with triethylamine effected the nitroaldol cyclization to give a mixture of diastereomeric racemic azepanols **19**. Reduction of the nitro group with zinc in the presence of hydrochloric acid gave amines **20**, which were coupled with *N*-Boc-*L*-leucine in the presence of EDC and HOBT to deliver amides **21**. Reductive removal of the *N*-benzyl moiety with hydrogen gas in the presence of 10 mol % Pd on carbon yielded secondary amines **22**. Sulfonylation with 2-pyridylsulfonyl chloride supplied sulfonamides **23**. Removal of the Boc group of **23** under acidic conditions, followed by EDC/HOBT coupling of the resulting amine salt with benzofuran-2-carboxylic acid, gave amides **24**. Oxidation of the alcohols with Dess–Martin periodinane provided an isomeric mixture of the azepanones **2, 3, 4**, and **5**. The *cis*-diastereomers, **2** and **5**, were separated from the *trans*-diastereomers, **4** and **3**, by HPLC using an Impaq silica gel column. Each pair of diastereomers was further subjected to an additional HPLC purification on a Chiracel OD column to obtain each individual azepanone in an isomerically pure form (>95% diastereomeric purity).

The 6- and 7-methyl-substituted azepanones **6–13** were prepared using ring-closing metathesis (RCM) strategies⁵ as shown in Schemes 2 and 3. Toward the preparation of 6-methylazepanone analogues (**6–9**), racemic 2-methylpent-4-enoic acid ethyl ester **25** was converted to aldehyde **26** by DIBAL-H reduction. Reductive amination with allylamine afforded secondary amine **27**. Sulfonylation with 2-pyridine-sulfonyl chloride provided sulfonamide **28**. Treatment of **28** with

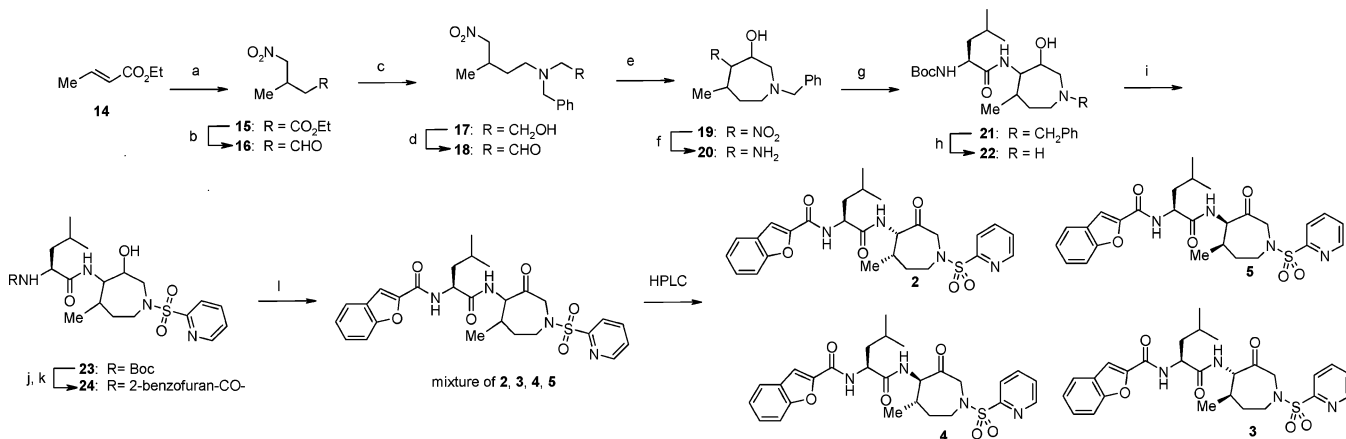
Grubbs' RCM catalyst, bis(tricyclohexylphosphine)benzylidineruthenium(IV) dichloride, gave azepine **29**. Epoxidation with *m*CPBA afforded a mixture of *syn*- and *anti*-epoxides **30** and **31** (~1:1 ratio), respectively, which were separated by column chromatography. Individual epoxides **30** and **31** were treated with sodium azide to regioselectively³ and stereospecifically afford azides **32** and **33**. Reduction of the azides with triphenylphosphine gave amines **34** and **35**. Acylation with *N*-Boc-*L*-leucine and HBTU furnished amides **36(a+b)** and **37(a+b)**. Deprotection of the Boc groups of **36(a+b)** and **37(a+b)** with HCl in dioxane followed by acylation with 2-benzofuran carboxylic acid using HBTU gave the intermediate alcohols **38(a+b)** and **39(a+b)**. Oxidation with Dess–Martin periodinane yielded a pair of mixtures of diastereomeric azepanones. Each pair of diastereomers was further purified by HPLC on an *R,R*-Whelk-O chiral phase column to afford the individual azepanones **6–9** in an isomerically pure form (>95% diastereomeric purity).

The sequence depicted in Scheme 3 was used for the synthesis of the 7-methyl-substituted azepanone analogues. Reductive amination of 5-hexen-2-one **40** with allylamine gave secondary amine **41**. Protection with carbobenzyloxy chloride gave diene **42**. Treatment with Grubbs' RCM catalyst gave azepine **43**. Epoxidation with *m*CPBA afforded a mixture of *anti*- and *syn*-epoxides **44** and **45** (3:1 ratio), respectively, which were separated by flash column chromatography. The epoxides were converted into azido alcohols **46** and **47** by reaction with sodium azide, along with the regioisomeric azido alcohol **48** which formed as an 18% impurity from **45**. The regio- and stereochemical assignments of **46** and **47** were determined by X-ray crystallography (ORTEPs and coordinates in Supporting Information). Reduction with triphenylphosphine produced primary amines **49** and **50**. Acylation with *N*-Boc-*L*-leucine and EDC/HOBT gave mixtures of amides **51(a+b)** and **52(a+b)**. Hydrogenolysis removed the Cbz groups to provide secondary amines **53(a+b)** and **54(a+b)**, which were sulfonylated with 2-pyridinesulfonyl chloride to give sulfonamides **55(a+b)** and **56(a+b)**. Treatment of **55(a+b)** and **56(a+b)** with HCl removed the Boc groups, and the resulting primary amines were acylated with 2-benzofuran carboxylic acid and EDC/HOBT to yield the alcohols **57(a+b)** and **58(a+b)**. Oxidation with Dess–Martin periodinane yielded a pair of mixtures of diastereomeric azepanones. Each pair of diastereomers was purified by HPLC using an *R,R*-Whelk-O chiral phase column to afford individual azepanones **10–13** in an isomerically pure form (>95% diastereomeric purity).

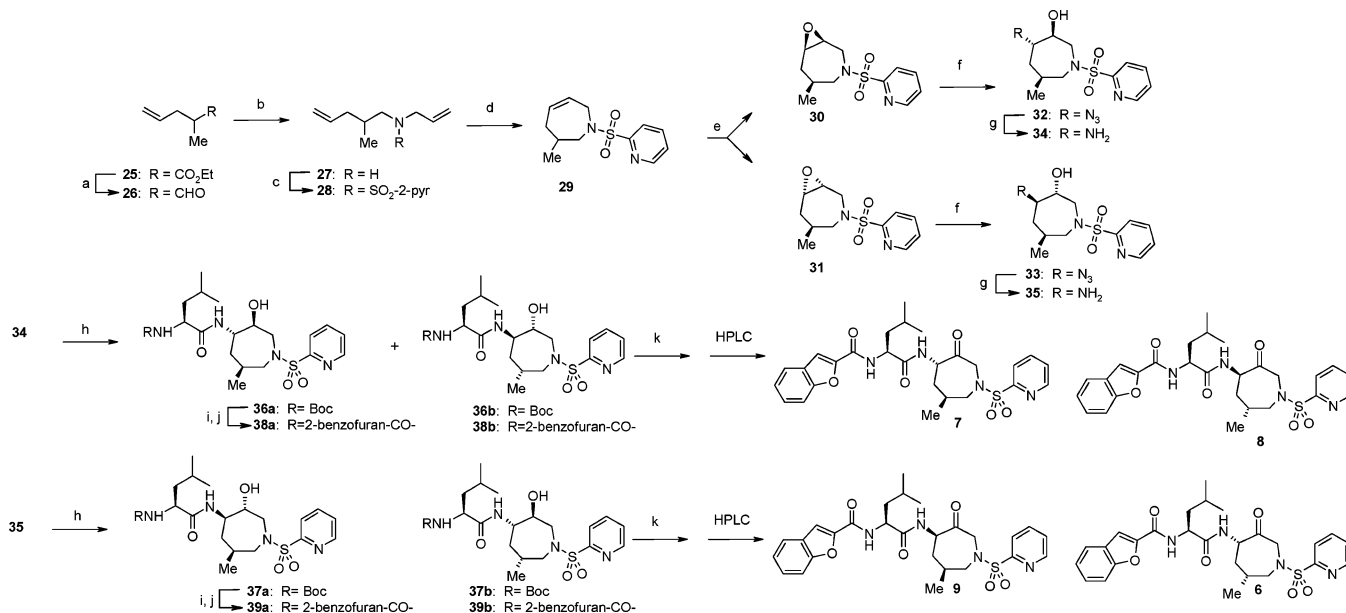
Physical and Structural Characterization of Azepanones

Small Molecule X-ray Crystallography. As an aid in the stereochemical assignments for the various diastereomeric azepanones, high-quality crystals of compounds **3, 5, 6**, and **10** were obtained and single-crystal X-ray structures were determined (ORTEPs and coordinates in Supporting Information). The ring dihedral angles of the unsubstituted azepanone **1** (ref 3, Supporting Information) along with the 5-methyl-substituted azepanones **3** and **5**, the 6-methyl-substituted azepanone **6**, and the 7-substituted azepanone **10** are listed in Table 2. By comparison to canonical dihedral angles of chair and twist-boat conformations of cycloheptane,⁶ **1, 3, 5**, and **6** crystallize in the same chair conformation, while **10** adopts a twist-boat conformation. In all four compounds examined, the amide group is oriented equatorially. In **3, 6**, and **10**, the methyl group assumes an equatorial orientation, while in **5**, the methyl group is in an axial orientation (Figure 2).

Epimerization Rates and Equilibria. The pH-dependent rates of epimerization of the C4 chiral center for **1**, its

Scheme 1. Synthesis of 5-Methylazepanones^a

^a Reagents: (a) MeNO₂, TMG; (b) DIBAL-H, toluene -78°C ; (c) Na(OAc)₃BH, N-benzylethanolamine; (d) oxalyl chloride, DMSO, -78°C ; (e) Et₃N, rt; (f) Zn, MeOH, HCl; (g) *N*-Boc-L-leucine, EDC, HOBT; (h) H₂, Pd/C; (i) 2-pyridinesulfonyl chloride, Et₃N; (j) HCl, dioxane; (k) 2-benzofurancarboxylic acid, EDC, HOBT, Et₃N; (l) Dess–Martin periodinane, CH₂Cl₂

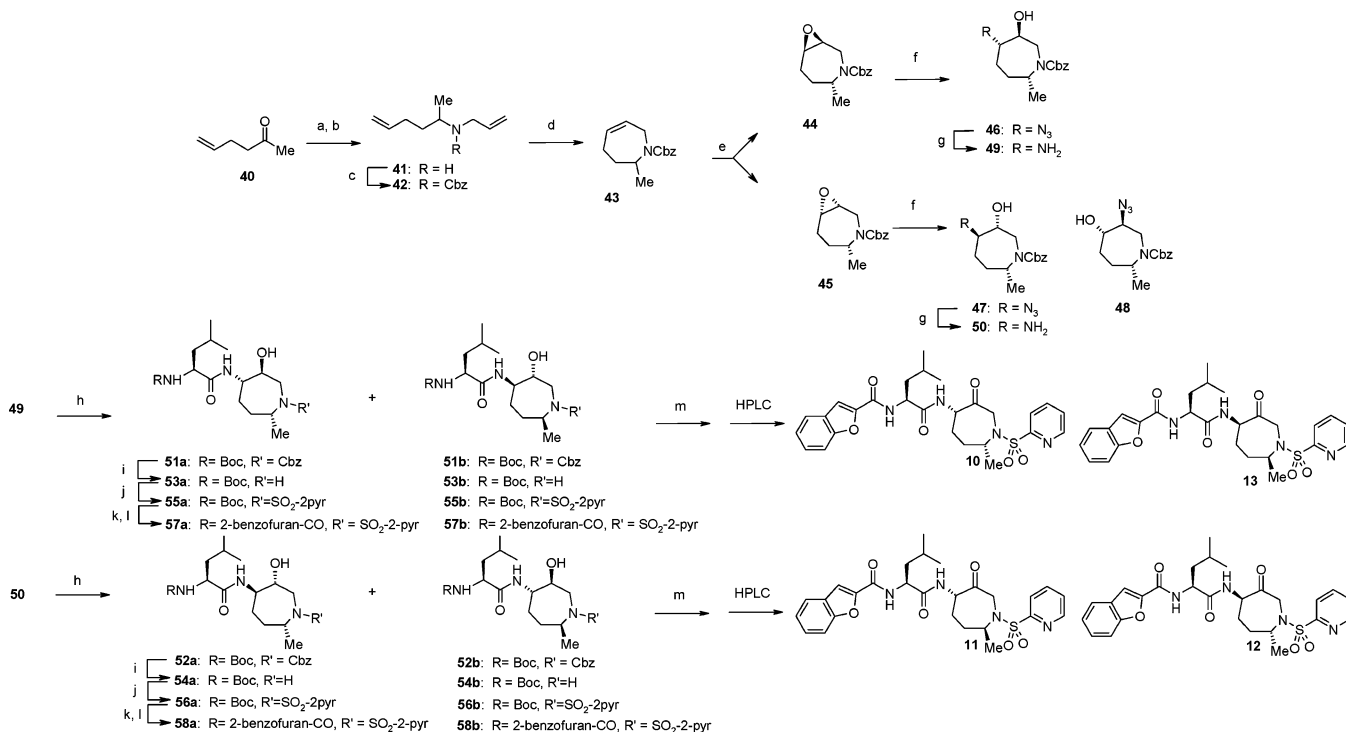
Scheme 2. Synthesis of 6-Methylazepanones^a

^a Reagents: (a) DIBAL-H, toluene -78°C ; (b) allylamine; CH₂Cl₂, NaBH₄; (c) 2-pyridinesulfonyl chloride, NMM; (d) bis(tricyclohexylphosphine)benzylidineruthenium(IV) dichloride, CH₂Cl₂; (e) *m*-CPBA, CH₂Cl₂; (f) sodium azide, MeOH, H₂O; (g) triphenylphosphine, THF, H₂O; (h) *N*-Boc-L-leucine, HBTU, NMM, DMF; (i) HCl, dioxane; (j) 2-benzofurancarboxylic acid, HBTU, NMM, DMF; (k) Dess–Martin periodinane, CH₂Cl₂.

corresponding C4 epimer, and their 2,2,4-trideuterated analogues were reported in ref 3. Similar HPLC methods, optimized for each pair of epimers, were developed to evaluate the effect of methyl substitution at C5 (**2**, **4**), C6 (**6**, **8**), and C7 (**11**, **13**) on the kinetics and steady-state ratios of the C4 epimers in aqueous phosphate buffer at pH 11. The C5-substituted compounds **2** and **4** epimerized at a slower rate than unsubstituted azepanone **1** and reached a 1:1 ratio from either direction. This slower rate was anticipated on the basis of the increased steric hindrance of the methyl group on the formation of the intermediate enolates.⁷ The epimerization rate constants increased as the methyl group was moved from C5 to C6 and to C7, approaching that of **1**. The C6 and C7 substituted compounds reached equilibrium strongly favoring one epimer over the other, as shown in Table 3. This reversible unsymmetrical epimerization is clearly illustrated in Figure 3, where the thermodynamic ratios of **2**⇌**4** and **11**⇌**13** are compared. Note that in the 7-methyl series, the *cis* diastereomer has the greater cathepsin K inhibitory potency (**10** vs **12**) as well as increased thermodynamic stability.

This increased thermodynamic stability is a fortuitous physical property because it facilitates synthesis and scale-up of **10** by allowing for conversion of mixtures of **10** and **12** to predominantly **10** by a simple epimerization process.

Structure Assignments. A combination of small molecule X-ray crystallography, epimerization studies, and NMR spectroscopic studies were utilized to obtain complete assignment of the structures of the isomeric compounds **2**–**12**. Representative azepanones substituted by a methyl group at each of the 5-, 6-, and 7- positions were elucidated by small-molecule crystallography as described above; the unambiguous assignment of the azepanone relative and absolute stereochemical configurations were as follows: **3** = 4*S*, anti; **5** = 4*R*, syn; **6** = 4*S*, syn; **10** = 4*S*, syn. The compounds were practically stable to epimerization at neutral pH, but when subjected to pH 11 buffered conditions, the diastereomers interconverted by C4 epimerization and were separable by HPLC (Scheme 4). Interconversion of **2** and **4**, **3** and **5**, **6** and **8**, **7** and **9**, **10** and

Scheme 3. Synthesis of 7-Methylazepanones^a

^a Reagents: (a) allylamine, pTsOH; (b) NaBH₄, MeOH; (c) carbobenzyloxy chloride, Et₃N, CH₂Cl₂; (d) bis(tricyclohexylphosphine)benzylidineruthenium(IV) dichloride, CH₂Cl₂; (e) mCPBA, CH₂Cl₂; (f) sodium azide, MeOH, H₂O; (g) triphenylphosphine, THF, H₂O; (h) *N*-Boc-L-leucine, EDC, HOBT, DMF; (i) H₂, Pd/C, MeOH; (j) 2-pyridinesulfonyl chloride, NMM; (k) HCl, dioxane; (l) 2-benzofurancarboxylic acid, HBTU, NMM, DMF; (m) Dess–Martin periodinane, CH₂Cl₂

Table 2. Dihedral Angles of **1**, **3**, **5**, **6**, **10**, Canonical Cycloheptane Chair (**C**), Canonical Cycloheptane Twist-boat (**TB**), 1/Cathepsin K Cocrystal (**1C**), and **10**/Cathepsin K Co-crystal (**10C**)

dihedral	1	3	5	6	10	C	TB	1C	10C
N1C2C3C4	9.4	-1.3	-3.2	8.5	6.1	0.0	17.9	-73	-70
C2C3C4C5	-71.7	-66.7	70.9	-72.0	-55.8	-66.1	-74.6	57	49
C3C4C5C6	82.2	82.5	-81.7	83.3	3.8	83.5	17.9	-67	0.4
C4C5C6C7	-60.4	-61.5	59.4	-60.3	72.5	-63.8	64.4	67	-53
C5C6C7N1	60.0	58.2	-60.7	59.5	-45.3	63.8	-45.4	-17	68
C6C7N1C2	-91.4	-86.6	92.1	-91.4	-50.8	-83.5	-45.4	-58	-68
C7N1C2C3	70.7	75.2	-73.9	69.8	76.6	66.1	64.4	92	75

12, and **11** and **13** allowed the unambiguous assignment of ketones **8** = 4*R*, anti and **12** = 4*R*, anti.

The remaining structures were assigned by proton NMR experiments. The structures of the two remaining 5-methylazepanones **2** and **4** were deduced from the methine C4 and C5 proton–proton coupling constants. Matching the corresponding syn and anti diastereomers **5** ($J = 2.1$ Hz) and **3** ($J = 8.5$ Hz), respectively, strongly suggested the assignments as **2** = 4*S*, syn ($J = 1.8$ Hz) and **4** = 4*R*, anti ($J = 8.9$ Hz). The remaining 6-methylazepanone assignments were made by proton NOE experiments. Compounds **6** and **9** (but not **7** and **8**) had NOE's between the C4 and C6 methine protons, consistent with **6** = 4*S*, syn and **9** = 4*R*, syn. Compounds **7** and **8** (but not **6** and **9**) had NOE's between the C4 methine and C6 methyl protons, consistent with **7** = 4*S*, anti and **8** = 4*R*, anti. Finally, the remaining 7-methylazepanone assignments were made by comparing the AB coupling of the C2 methylene protons. Compounds **10** and **13** had the same coupling constant ($J_{AB} = 19.4$ Hz), consistent with **13** = 4*R*, syn, whereas **11** and **12** had the same coupling constant ($J_{AB} = 17.7$ Hz), consistent with **11** = 4*S*, anti.

Conformational Analysis. To assess the solution structures of **1**, **2**, **7**, and **10** for comparison with the bound conformations

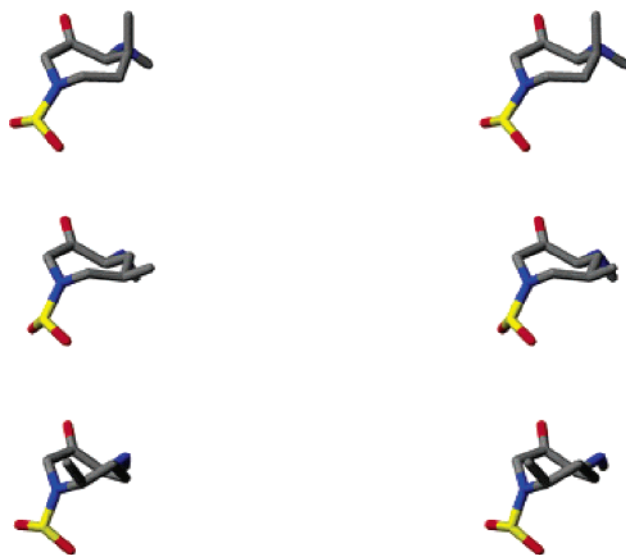


Figure 2. Stereoview comparison of the azepanone cores and substituents of **5** (enantiomer depicted, top), **6** (middle), and **10** (bottom) determined by single-crystal X-ray diffraction. Note the axial methyl group of **5** (enantiomer depicted).

of **1** and **10**, the NAMFIS (NMR analysis of molecular flexibility in solution) procedure was employed.⁸ Briefly, the NAMFIS method computationally identifies the family of conformers that best fit NMR-determined NOE and $^3J_{HH}$ coupling constants. The rationale is that a small flexible molecule most likely does not exist as a single conformation in solution but rather as a population of energetically accessible conformers. Rather than calculating conformer populations or mole fractions from force field energies, which are especially unreliable for druglike molecules with multiple long-range polar functionalities, the computation selects only conformers for

Table 3. Inhibition Constants, Physical Properties, and in Vitro Antiresorptive Potency

no.	cathepsin $K_{i,app}$ (nM)					rat: K	MW (Da)	clog P ^a	no. H-bond donor/acceptor	PSA (Å ²) ^b	nRot	epimerization		IC ₅₀ (nM) ^d
	K	L	V	S	B							thermo ratio	k (1/s) ^c	
1	0.16	2.2	1.8	4.0	500	60	526.61	3.08	2/9	138.68	8	6.2×10^{-5}	1:1	63
2	0.0099	0.040	ND ^e	ND	32	ND	540.64	3.60	2/9	138.68	8	2.6×10^{-5}	1:1	20
3	1.5	4.2	ND	ND	>1000	ND	540.64	3.60	2/9	138.68	8	ND	ND	ND
4	19	52	ND	ND	>1000	ND	540.64	3.60	2/9	138.68	8	3.4×10^{-5}	1:1	ND
5	42	45	ND	ND	>1000	ND	540.64	3.60	2/9	138.68	8	ND	ND	ND
6	29	160	ND	350	ND	>1000	540.64	3.60	2/9	138.68	8	ND	ND	ND
7	0.14	0.63	ND	5.8	ND	73	540.64	3.60	2/9	138.68	8	3.9×10^{-5}	1:5	35
8	30	150	ND	300	ND	>1000	540.64	3.60	2/9	138.68	8	ND	ND	ND
9	4.5	10	ND	8.3	ND	660	540.64	3.60	2/9	138.68	8	1.8×10^{-4}	5:1	ND
10	0.041	0.068	0.063	1.6	13	8.0	540.64	3.60	2/9	138.68	8	ND	9:1	22
11	2.5	7.9	ND	42	ND	680	540.64	3.60	2/9	138.68	8	6.5×10^{-5}	9:1	ND
12	1.4	4.5	ND	92	ND	430	540.64	3.60	2/9	138.68	8	ND	1:9	ND
13	4.0	3.9	ND	110	ND	790	540.64	3.60	2/9	138.68	8	6.0×10^{-4}	1:9	ND

^a Daylight Chemical Information Systems, version 4.71. ^b PSA = polar surface area. ^c At pH 11 ^d Osteoclast resorption assay. ^e ND = not determined.

Table 4. Populations of Axial Conformations from 10 000-Step Monte Carlo Conformational Searches with the MMFFs/CHCl₃ Protocol (8 kcal/mol Cutoff)

ketone MeSH methyl thiohemiketal

no.	molecular form	no. axial conformers < 8 kcal/mol	no. total conformers < 8 kcal/mol	fraction axial	K_i (nM)
1	azepanone	161	848	0.190	0.16
	thiol-reacted	245	1298	0.189	
2	azepanone	201	817	0.246	0.0099
	thiol-reacted	607	1296	0.468	
3	azepanone	61	627	0.097	1.5
	thiol-reacted	102	1432	0.071	
7	azepanone	220	836	0.263	0.14
	thiol-reacted	466	1424	0.327	
10	azepanone	96	1149	0.084	0.041
	thiol-reacted	279	1480	0.189	

which mole fractions are determined from the NMR data. The resulting conformer populations were analyzed to assess ring conformations as well as substituent orientations. This analysis revealed that the mole fractions of twist-boat conformations of **1**, **2**, **7**, and **10** were 0.10, 0.02, 0.26, and 0.31, respectively. Therefore, the predominant conformations of all four compounds examined were chair, and **2** had very little twist-boat present. In addition, substituent orientations were very similar for all four azepanone solution conformer populations. In all of the cases examined, the amide adopted an equatorial orientation with no evidence of axial amide orientations within the detection limits of proton NMR, even though axial amide orientations were available in the conformer set used as input to the NAMFIS procedure.

For the purpose of exploring the potential relationships between cathepsin K inhibitory potencies and calculated axial

conformer populations, conformational searches were carried out for azepanones **1**, **2**, **3**, **7**, and **10** and their methyl thiohemiketal counterparts (simple models of active site cysteine–inhibitor complexes) (Table 4). Of the five compounds examined, compound **2** with a *cis*-5-methyl group, is the most potent cathepsin K inhibitor ($K_i = 0.0099$ nM) and has calculated axial conformer populations of 25% and 47% for the ketone form and the methyl thiohemiketal form, respectively. The *trans*-5-methyl isomer **3** is the least potent inhibitor examined in this set ($K_i = 1.5$ nM) and has only 10% and 7% of its calculated axial conformer population for the ketone and methyl thiohemiketal forms, respectively. Compound **1**, with no methyl substitution, has an intermediate level of inhibitory potency ($K_i = 0.16$ nM) and has an intermediate level of calculated axial conformer populations of 19% for both ketone and methyl thiohemiketal forms. The *trans*-6-methyl analogue **7** has approximately the same inhibitory potency ($K_i = 0.14$ nM) as compound **1** and has calculated axial conformer populations for both ketone and methyl thiohemiketal forms comparable to compound **1**. However, the *cis*-7-methyl analogue **10**, the second most potent inhibitor of this set of compounds ($K_i = 0.041$ nM), has a calculated axial conformer population of only 8% for the ketone form and 19% for the methyl thiohemiketal form, lower than expected on the basis of the other calculated results. So, while the conformational analysis employed here demonstrates that compounds with larger calculated axial conformer populations (in either the ketone form or as the methyl thiohemiketal form) have greater enzyme inhibitory potency, this trend does not hold for compound **10**, and, therefore, cannot be used to fully rationalize the enzymology results.

Cathepsin K X-ray Cocrystallography. High-quality crystals of inhibitor **10** bound to cathepsin K were obtained by the vapor diffusion method. The structure was determined by molecular replacement with a model consisting of all protein atoms from the previously determined cathepsin K/E-64 complex (PDB ID 1ATK),⁹ and the structure was refined to 2.5-Å resolution. In Figure 4 is shown the X-ray cocrystal structure of **10** in the cathepsin K active site. The hydrophobic surface (green), hydrophilic surface (blue), and active lone pairs (magenta) are depicted. Compound **10** adopts a chair conformation (Table 2), and both the amide and the methyl groups are oriented axially. The orientation of these groups is in dramatic contrast to the preferred diequatorial conformations as observed in a single molecule X-ray structure. Clearly, the inhibitor

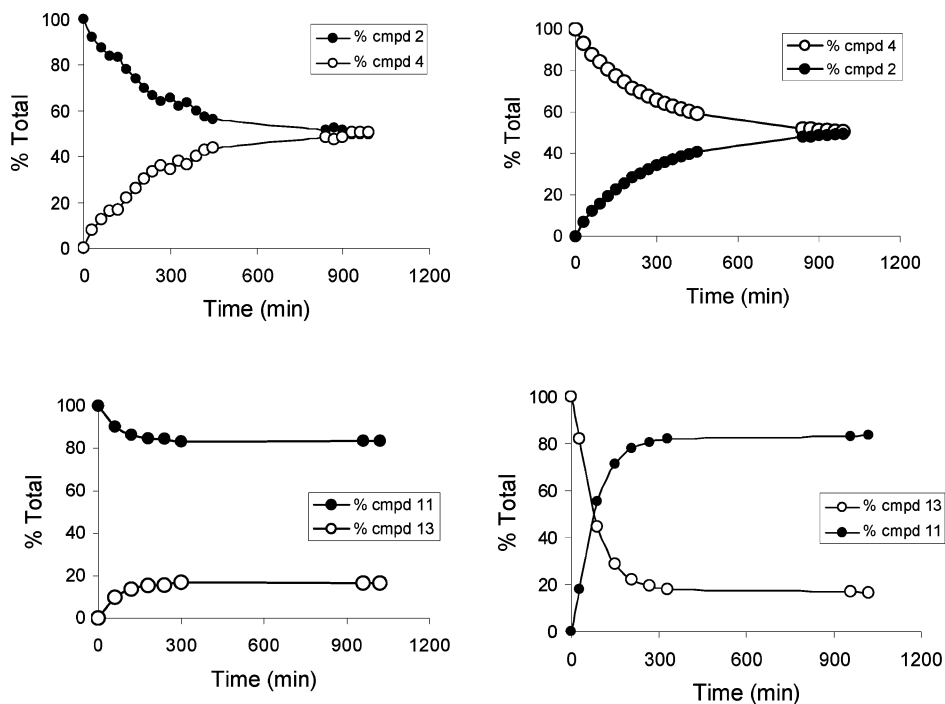
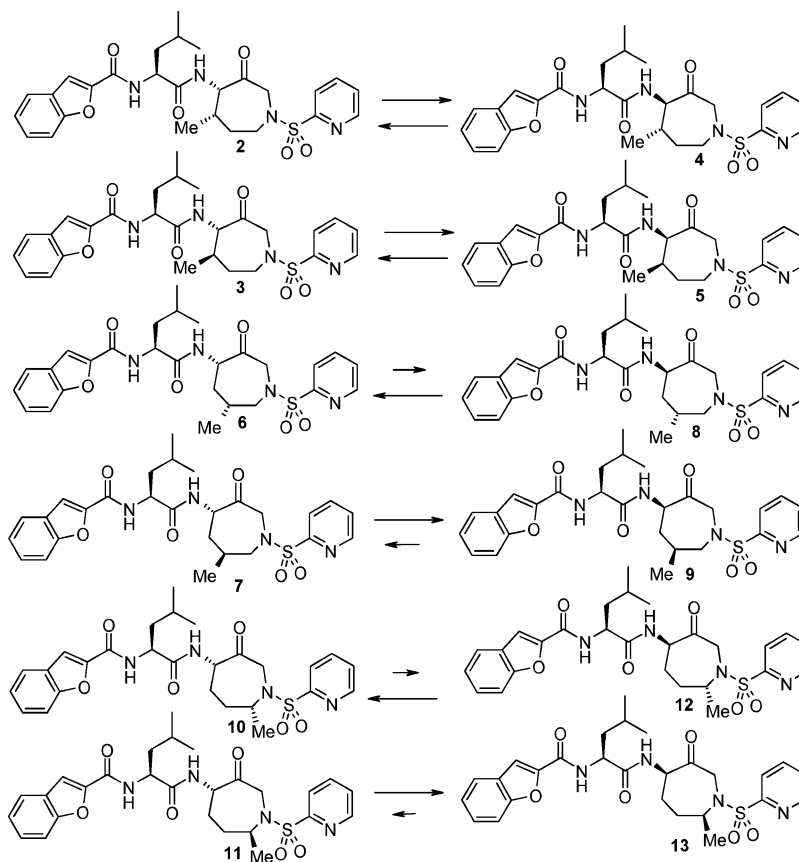


Figure 3. Percent total of the epimer left or formed vs the elapsed time after the addition of (from left to right, top to bottom) **2**, **4**, **11**, and **13**, respectively. The epimer concentrations at different times were determined by reverse-phase HPLC methods.

Scheme 4. Interconversion of 5-, 6-, and 7-Methylazepanone Diastereomers at pH 11 by Epimerization



undergoes a conformational change on binding to the enzyme. In addition, the axial methyl group of **10** makes contacts with the top of the S1' hydrophobic pocket, and the pyridine ring binds in the S2' hydrophobic pocket. A comparison with the cathepsin K/1 cocrystal structure will be described in the Discussion and Conclusions section.

Biological and Biochemical Characterization of Azepanones

Cathepsin Inhibition SAR. The rank order of cathepsin K inhibitory potency of the 4*S* diastereomers is 5-*cis*-methylazepanone (**2**, Table 3, $K_{i,app} = 0.0099$ nM) > 7-*cis*-methylazepanone (**10**, $K_{i,app} = 0.041$ nM) > 6-*trans*-methylazepanone (**7**, $K_{i,app} = 0.14$ nM) = parent azepanone (**1**, $K_{i,app} = 0.16$ nM).

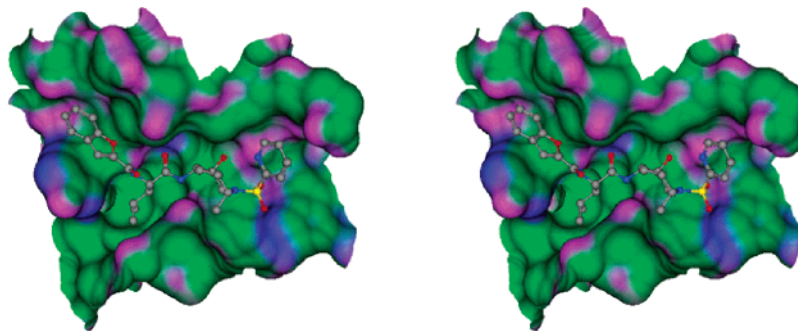


Figure 4. Stereoview of cathepsin K active site cocrystallized with **10** (hydrophobic surface green, hydrophilic surface blue, and hydrogen bond donor/acceptor surface magenta).

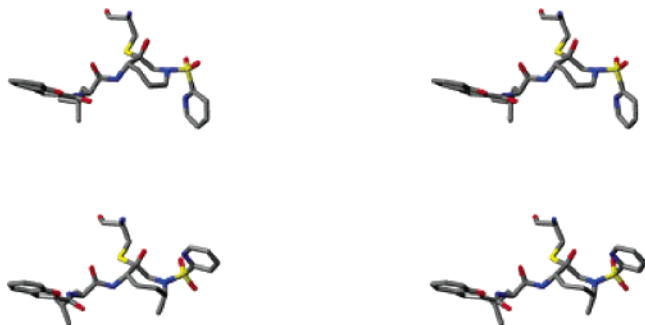


Figure 5. Stereoview comparison of **1** (top) and **10** (bottom) in cathepsin K-bound conformations.

In the 5-methyl series, the *cis*-4*S*-diastereomer **2** was >150-fold more potent than the *trans*-4*S*-diastereomer **3**, and **2** was the most potent cathepsin K inhibitor identified in this study. In the 6-methyl series, the *trans*-4*S*-diastereomer **7** was >200-fold more potent than the *cis*-4*S*-diastereomer **6**. In the 7-methyl series, the *cis*-4*S*-diastereomer **10** was >60-fold more potent than the *trans*-4*S*-diastereomer **11**. The 4*R*-diastereomers had much poorer cathepsin K inhibitory potency (>30-fold) than the 4*S*-diastereomers, as was also noted in ref 3 comparing **1** with its 4*R*-epimer. Quantification of the $K_{i,app}$ s of the 4*R*-diastereomers may have been limited by the inability to completely purify the samples free of their corresponding, much more potent 4*S*-counterparts (although >95% purity was achieved as measured by analytical HPLC). Compound **10** was generally a less selective inhibitor than **1** and had increased inhibitory potency vs human and rat cathepsin K, human cathepsins L and V, and especially vs human cathepsin B (Table 3). Despite this reduced selectivity, the improved pharmacokinetic and development characteristics of **10** discussed below led to its choice as candidate for human clinical trials.

In Vitro Biological Activity. The most potent diastereomers from each azepanone regioisomeric series (**1**, **2**, **7**, and **10**) were tested in the in vitro osteoclast resorption assay.¹⁰ Briefly, in this assay compounds are incubated for 48 h at a range of concentrations with human osteoclastoma-derived osteoclasts seeded onto bovine cortical bone slices. The production of type-I collagen C-telopeptides is measured using a commercial ELISA assay (Osteometer Biotech, Herlev, Denmark). The mean IC_{50} of **1** was 63 nM (Table 3, $n = 8$, standard deviation = 29 nM). Compounds **2**, **7**, and **10** had IC_{50} s ranging from 20 to 35 nM (Table 3, $n = 1$). Given that the IC_{50} s in this assay can vary as much as ~3-fold,¹⁰ these activities are considered to be approximately equivalent.

Pharmacokinetics, Plasma Protein Binding, and Cell and Membrane Permeability. The most potent diastereomers from each azepanone regioisomeric series (**1**, **2**, **7**, and **10**) were evaluated in pharmacokinetic iv/po crossover studies in rats (n

= 3). The substitution of a methyl group on the azepanone ring had remarkable and unpredictable effects on oral bioavailability, clearance, and half-life in the rat (Table 5). Unsubstituted azepanone **1** was a moderate clearance molecule and had a half-life of 30 min with a volume of distribution three times total body water. Oral bioavailability of **1** was 42%. In contrast, 5-*cis*-methyl analogue **2**, the most potent inhibitor of cathepsin K, was rapidly cleared yet had a half-life of 59 min, probably related to a volume of distribution approximately 7 times total body water. Following oral administration, measurable concentrations were observed at only one time point in one animal. Therefore, the oral bioavailability of **2** was below the lower limit of sensitivity of the test system (<5.4%). The 6-*trans*-methyl analogue **7** was cleared at a moderate rate with a half-life of about 52 min and a volume of distribution approximately double that of total body water. The oral bioavailability of **7** was 26%. The 7-*cis*-methyl analogue **10** was a low to moderate clearance molecule in the rat with a half-life of about 109 min and a volume of distribution approximately twice total body water. The oral bioavailability of **10** was outstanding at 89% in the rat, the highest we had seen of the compounds described here.

Compounds **1** and **10** were also evaluated in pharmacokinetic iv/po crossover studies in monkeys. Compound **1** was a low to moderate clearance molecule in the monkey with a half-life of 36.5 min and a volume of distribution approximately equal to total body water. The oral bioavailability of **1** was 7% in the monkey. Compound **10** had a low rate of clearance in the monkey and a half-life of 168 min with a volume of distribution approximately equal to total body water. The oral bioavailability of **10** was 28% in the monkey.

The percent rat plasma protein binding of **1**, **2**, **7**, and **10** was determined by either equilibrium dialysis or ultrafiltration and ranged from 95% to 97% (Table 5). Also, permeation rates in Madin–Darby canine kidney (MDCK) cells and in an artificial black-lipid membrane assay¹¹ were quantified (Table 5). No significant differences were observed between the compounds. It is therefore unlikely that protein binding, renal clearance, or membrane permeation rate play a significant role in the pharmacokinetic differences observed for these compounds.

Discussion and Conclusions

Attempts to rationalize the differences in cathepsin K inhibitory potencies of the various methyl-substituted azepanone inhibitors relative to the conformational accessibility of the equatorial vs axial amide orientations were made, as this had been an initial goal of preparing these isomeric series. The 4*S*-5-*trans*-methyl analogue (**3**), the 4*S*-6-*cis*-methyl analogue (**6**),

Table 5. Rat and Monkey Pharmacokinetic Parameters, Rat Plasma Protein Binding, Cell and Membrane Permeability

no.	rat (monkey)				permeability ($\times 10^{-5}$ cm/s)		
	iv				% plasma protein binding	MDCK	artificial membrane
	$T_{1/2}$, min	CL, mL/min/kg	Vd _{ss} , L/kg	po: %F			
1	29.8 \pm 2.22 (36.5 \pm 0.06)	49.2 \pm 4.5 (13.9 \pm 3.4)	1.86 \pm 0.36 (0.72 \pm 0.20)	42.1 \pm 19.8 (7.3 \pm 4.7)	97.0 \pm 0.1	5.7	5.3
2	58.5 \pm 21.8	80.5 \pm 16.5	4.70 \pm 2.16	<5.4 ND ^a	94.7 \pm 1.5	5.5	6.8
7	51.6 \pm 12.2	34.4 \pm 2.9	1.46 \pm 0.20	26.2 \pm 10.2	95.6 \pm 0.1	4.9	5.6
10	109 \pm 8.0 (168 \pm 25)	19.5 \pm 4.0 (11.7 \pm 3.1)	1.79 \pm 0.50 (0.95 \pm 0.38)	89.4 \pm 32.3 (27.6 \pm 3.5)	96.8 \pm 0.3	4.7	4.7

^a ND = not determined.

and the 4*S*-7-*trans*-methyl analogue (**11**) were 60 to >200-fold less potent than their corresponding 4*S*-5-*cis*-methyl analogue (**2**), 4*S*-6-*trans*-methyl analogue (**7**), and 4*S*-7-*cis*-methyl analogue (**10**). In addition, **2** and **10** were more potent cathepsin K inhibitors than the parent azepanone **1**. We had hypothesized that the solution population of axial vs equatorial amides might vary with methyl group substitution of the azepanone ring. However, the results of the NAMFIS conformational study revealed that there were no axial amides present with **1**, **2**, **7**, or **10** in solution within the detection limits of proton NMR. Therefore, this hypothesis is inconsistent with the experimental data.

An alternative hypothesis was considered in which methyl substitution might alter the energy required to interconvert the equatorial and axial amide orientations. In cases where methyl substitution stabilizes the equatorial amide, the cathepsin K inhibitory potency should be decreased; in cases where the methyl group destabilizes the equatorial amide, the cathepsin K inhibitory potency should be increased. Indeed, in both sets of 4*S*-5- and 6-methylazepanone analogues, the differences in potency of **3** vs **2** and **6** vs **7** can be rationalized by this hypothesis. Both **3** and **6** should have greater stabilization of diequatorial chair conformers relative to the diaxial chair conformers, and both **2** and **7** should require a lower energy of interconversion of the two axial–equatorial chair conformers. However, in the case of the 7-methyl analogues, this hypothesis is not consistent with the observed potencies. Compound **10** should have greater stabilization of the diequatorial chair conformer relative to the diaxial chair conformer, but was a more active cathepsin K inhibitor than **1**; compound **11** should require a lower energy of interconversion of the two axial–equatorial chair conformers, but was a less potent cathepsin K inhibitor than **1**.

The X-ray cocrystal structure of **10** bound to cathepsin K provided a plausible explanation for this disparity with the 7-methylazepanone analogues. When bound to cathepsin K, **10** adopts a chair conformation (**10C**, Table 2) with both the amide and the methyl group adopting axial orientations. The methyl group of **10** occupies the S1' hydrophobic pocket of the enzyme, and the pyridine ring interacts with the S2' hydrophobic pocket (Figure 4). With compound **1**, the pyridine ring occupies the S1' hydrophobic pocket and forms an aromatic–aromatic interaction with Trp184. Therefore, it appears that favorable interactions with the enzyme counteracted the unfavorable diaxial chair conformation of **10**. Furthermore, the methyl group of **10** affords an additional interaction with the enzyme that cannot be accessed by the methyl group of the epimeric analogue **11**.

The difference in orientation of the pyridine ring of **10** vs **1** in the cathepsin K cocrystal structures (Figure 5) also provided insight into the differences in cathepsin B selectivity between

10 ($K_{i,app} = 13$ nM) and **1** ($K_{i,app} = 500$ nM). Cathepsin K–**1** and –**10** cocrystal structures were aligned with a publicly available cathepsin B crystal structure (PDB ID 1CSB).¹² In both cathepsin K and cathepsin B, the S1' binding pockets are delineated by a β strand (residues 162–166 in cathepsin K and residues 197–203 in cathepsin B). In cathepsin B, this β strand is shifted relative to cathepsin K, reducing the size of the S1' pocket. We speculate that this reduced size of S1' in cathepsin B results in a poor fit of the pyridine of **1** due to steric clashes. Furthermore, compound **1** lacks a 7-*cis*-methyl group and therefore does not form this hydrophobic interaction with S1' of cathepsin B. In addition, it is plausible that **10** would bind to cathepsin B in an analogous fashion to its binding mode to cathepsin K and would therefore make favorable interactions with the cathepsin B S1' and S2' pockets.

The 4*S*-5-*cis*-methylazepanone analogue, **2**, had <5.4% rat oral bioavailability and had a rat in vivo clearance rate of 80.5 mL/min/kg, while the 4*S*-7-*cis*-methylazepanone analogue, **10**, had 89% rat oral bioavailability and a rat in vivo clearance rate of 19.5 mL/min/kg. On the basis of the lack of differentiation of **2** and **10** in plasma protein binding and in cellular and membrane permeability assays, it is likely that the differences in oral bioavailability are due to altered rates or efficiency of first-pass hepatic extraction and/or metabolism. We considered several hypotheses that might rationalize the differences in the pharmacokinetic profiles. One simple explanation is a steric hypothesis, in which the 7-methyl group sterically blocks sites of metabolism. Another explanation is a ring conformation hypothesis, in which compound **2** can readily access azepanone ring conformations that are readily recognized by in vivo first pass clearance systems (P-glycoproteins, CYP450s, proteases, etc.), and compounds such as **10** cannot readily access the same conformations. The small molecule crystal structure of **10** revealed that it crystallized in a twist-boat conformation (Table 2). On the basis of this small molecule X-ray structure, it was worth considering whether chair azepanone conformations might be well recognized by in vivo clearance systems and twist-boat conformations might be poorly recognized. However, on the basis of the NAMFIS study results, azepanones **1**, **2**, **7**, and **10** all adopted predominantly chair conformations in solution, and compounds **7** and **10** were not largely differentiated in their mole fraction of twist-boat populations (26% vs 31%, respectively). Obviously, the chair vs twist-boat hypothesis is too simplistic, since in an azepanone system there are a large number of possible chair and twist-boat conformations that are potentially accessible. For instance, in the various X-ray crystallography studies (Table 2), three different chair conformations and a twist boat conformation were observed: the same chair in four of the small molecule structures of **1**, **2**, **5**, and **6**; a different chair in the cathepsin K–**1** cocrystal structure; yet

another chair in the cathepsin K-**10** cocrystal structure; and a twist-boat in the small molecule X-ray structure of **10**. It is possible that a more sophisticated analysis of particular azepanone chair and twist-boat conformations accessible by compounds such as **2** and **10** might begin to rationalize the in vivo pharmacokinetic results.

In addition to preferred conformations, we also considered a compound rigidity hypothesis as another way to rationalize the differences in observed oral bioavailabilities of compounds **1**, **7**, and **10**. In a previous study of a diverse set of compounds ($n = 1117$), a high probability of good oral bioavailability ($>20\%$) in the rat was observed with compounds with a rotatable bond count (nRot) of less than 8.¹³ All of the azepanones discussed here have a nRot = 8 and therefore lie at or near an inflection point between high and low probability of good oral bioavailability. In general, methyl substitution of the azepanone should further decrease the overall ring flexibility, even though rings are wrongly assumed to be inflexible (nRot = 0) in this simple model. 7-Methyl substitution of the azepanone should decrease the rotational freedom of the 4-sulfonamide substituent. We speculate that these decreases in rotational freedom might rationalize the difference of oral bioavailability of **10** compared to **1**. 6-Methyl substitution should have little influence on the rotational freedom of the ring substituents, and indeed, the *trans*-6-methyl isomer **7** is most like **1** in pharmacokinetic properties. 5-Methyl substitution should decrease the rotational freedom of the 4-amide substituent. Despite having decreased compound flexibility, **2** has decreased oral bioavailability.

One particularly interesting aspect of the compounds described in this paper is that they are not largely differentiated by simple calculated diversity metrics (Table 3) such as Lipinski's rule-of-five (molecular weight, clog P, number of hydrogen bond donors or acceptors),¹⁴ number of rotatable bonds,¹³ or polar surface area.¹⁵ However, the effects on the compound properties that matter most to medicinal chemists, namely, potency and in vivo pharmacokinetic parameters such as oral bioavailabilities and clearance rates, were profound. Given the close structural similarity of **2** and **10**, we speculate that subtle conformational differences of the azepanone rings are giving rise to the differences in pharmacokinetic parameters. In addition, these examples demonstrate the potential for modulation of pharmacological properties of cathepsin inhibitors by substituting an azepanone core. Furthermore, such precedents emphasize the importance of the continued use of in vivo pharmacokinetic screening in the drug discovery process. The high potency for inhibition of cathepsin K coupled with the favorable rat and monkey pharmacokinetic characteristics of compound **10**, also known as SB-462795 or relacatib, has made it the subject of considerable in vivo evaluation for safety and efficacy as an inhibitor of excessive bone resorption in rat, monkey, and human subjects. Results of these numerous in vivo studies will be reported elsewhere.

Experimental Section

General. Except where indicated, materials and reagents were used as supplied. NMR spectra for compound characterization were recorded at 400 MHz using a Bruker AC 400 spectrometer. Mass spectra were taken on a PE Sciex API III instrument using electrospray (ES) ionization techniques. Elemental analyses were obtained using a Perkin-Elmer 240C elemental analyzer. Reactions were monitored by TLC analysis using Analtech silica gel GF or E. Merck silica gel 60 F-254 thin layer plates. Flash chromatography was carried out on E. Merck Kieselgel 50 (230–400 mesh) silica gel. Preparative and analytical HPLC were carried out on either the Rainin HPXL or Gilson 306 HPLC systems.

5-Methylazepanones. 3-Methyl-4-nitrobutyric Acid Ethyl Ester (15). To a solution of ethyl 2-crotonate **14** (10 g, 87 mmol) in nitromethane (23 mL, 438 mmol) was added 1,1,3,3-tetramethylguanidine (2.0 g, 17 mmol). The solution was stirred at room temperature for 24 h. Ether (500 mL) was added and the organic solution was washed with 1 N HCl (100 mL) and dried over sodium sulfate. The solution was filtered, concentrated, and purified on a silica gel column (20–30% EtOAc/hexane) to yield the title compound (14 g, 91%): ¹H NMR (CDCl₃) δ 4.50 (dd, $J = 12.1$, 6.2 Hz, 1H), 4.38 (dd, $J = 12.1$, 7.2 Hz, 1H), 4.18 (q, $J = 7.1$ Hz, 2H), 2.86–2.77 (m, 1H), 2.47 (dd, $J = 16.1$, 6.7 Hz, 1H), 2.38 (dd, $J = 16.1$, 6.9 Hz, 1H), 1.29 (t, $J = 7.1$ Hz, 3H), 1.13 (d, $J = 6.8$ Hz, 3H); MS (ESI) 174.0 (M+H)⁺.

3-Methyl-4-nitrobutyraldehyde (16). To a solution of 3-methyl-4-nitrobutyric acid ethyl ester **15** (1.0 g, 5.71 mmol) in dry toluene at –78 °C was slowly added DIBAL-H (4 mL, 1.5 M solution in toluene) so as to maintain the internal temperature below –65 °C. The reaction was stirred for 2 h at –78 °C. The reaction was then quenched by slowly adding cold (–78 °C) MeOH while the internal temperature was kept below –65 °C. The resulting white emulsion was slowly poured into ice-cold 1N HCl with swirling over 15 min and the aqueous mixture was then extracted with EtOAc (3×). The combined organic solution was washed with brine, dried over sodium sulfate, and concentrated to give the crude product which was then purified on a silica gel column (25% EtOAc/hexane) to give the pure product as a pale yellow oil (0.73 g, 98%): ¹H NMR (CDCl₃) δ 9.79 (s, 1H), 4.45 (dd, $J = 12.0$, 6.4 Hz, 1H), 4.38 (dd, $J = 12.0$, 6.0 Hz, 1H), 2.94–2.85 (m, 1H), 2.69 (dd, $J = 18.2$, 6.1 Hz, 1H), 2.55 (dd, $J = 18.2$, 7.0 Hz, 1H), 1.13 (d, $J = 6.9$ Hz, 3H).

2-[Benzyl(3-methyl-4-nitrobutyl)amino]ethanol (17). To a solution of 3-methyl-4-nitrobutyraldehyde **16** (0.73 g, 5.57 mmol) in CH₂Cl₂ (6.0 mL) were added sodium triacetoxylborohydride (1.57 g, 7.40 mmol) and *N*-benzylethanolamine (0.55 g, 3.67 mmol) at room temperature. The reaction was stirred for 16 h, whereupon it was quenched with water, diluted with EtOAc, and washed with aqueous NaHCO₃ and brine. The organic layer was dried over sodium sulfate, concentrated, and used directly in the next reaction: ¹H NMR (CDCl₃) δ 7.41–7.29 (m, 6H), 4.29–4.19 (m, 2H), 3.69–3.59 (m, 4H), 2.79–2.31 (m, 4H), 1.61–1.39 (m, 4H), 0.97 (d, $J = 6.9$ Hz, 3H); MS (ESI) 265.3 (M + H)⁺.

1-Benzyl-5-methyl-4-nitroazepan-3-ol (19). To a stirring solution of oxalyl chloride (2 M in CH₂Cl₂) (3.38 mL) in CH₂Cl₂ at –78 °C was added DMSO (1.25 mL, 17.6 mmol) slowly. After stirring for 15 min, a solution of alcohol **17** (0.60 g, 2.25 mmol) in CH₂Cl₂ (1 mL) was added slowly. The reaction was continued for a further 1 h at –78 °C to form the aldehyde **18** in situ. Triethylamine (4.7 mL, 33.8 mmol) was added, the reaction mixture was brought to room temperature and quenched with water, and the product was extracted into CH₂Cl₂. The organic layer was dried over sodium sulfate, filtered, and concentrated. To the crude product in THF was added triethylamine and the mixture stirred for 16 h at room temperature. The crude product was purified on a silica gel column (1–3% MeOH/DCM) to give title compound as a mixture of diastereomers (0.4 g, 41%, two steps): ¹H NMR (CDCl₃) δ 7.39–7.21 (m, 5H), 4.29–4.19 (m, 2H), 3.8 (s, 2H), 2.98–2.51 (m, 5H), 1.87–1.79 (m, 2H), 1.10 (d, $J = 6.7$ Hz, 3H); MS (ESI) 265.24 (M + H)⁺.

4-Amino-1-benzyl-5-methylazepan-3-ol (20). To a solution of MeOH (56 mL) and 12 N HCl (5.6 mL) was slowly added Zn dust (0.43 g, 6.47 mmol). Nitroazepanol **19** (171 mg, 0.65 mmol) was added and the reaction was heated to reflux for 18 h, whereupon it was concentrated in vacuo to remove the MeOH. The residue was diluted with EtOAc and water and made basic with solid KOH. The mixture was washed with brine, dried over sodium sulfate, filtered, and concentrated to give the title compound as a mixture of diastereomers (120 mg, 80%): MS (ESI) 235.2 (M + H)⁺.

[(S)-1-(1-Benzyl-3-hydroxy-5-methylazepan-4-ylcarbonyl)-3-methylbutyl]carbamic Acid *tert*-Butyl Ester (21). To a solution of the crude aminoazepanols **20** (1.12 g, 4.76 mmol) in CH₂Cl₂ (20 mL) were added Boc-L-leucine (1.3 g, 4.76 mmol), EDC (1 g,

4.76 mmol), and HOBT (0.13 g, 0.96 mmol). This mixture was stirred at room temperature for 3 h, whereupon it was diluted with EtOAc and washed with an aqueous solution of sodium bicarbonate. The organic layer was dried over sodium sulfate, filtered, and concentrated. The crude product was purified on a silica gel column (50% EtOAc/hexane) to remove polar impurities, and the mixture of diastereomers was carried on to the next reaction (0.12 g, 28%): MS (ESI) 448.4 (M + H)⁺.

[(S)-1-(3-Hydroxy-5-methylazepan-4-ylcarbamoyl)-3-methylbutyl]carbamic Acid *tert*-Butyl Ester (22). To a solution of amides **21** (10 g, 22.4 mmol) in MeOH and EtOAc (10 mL, 1:3) was added 10% Pd/C (2 g, 1.88 mmol) at room temperature. This mixture was shaken for 16 h on a Parr hydrogenation apparatus at 45 psi of hydrogen gas. The reaction mixture was filtered through a pad of Celite and concentrated to give the title compound which was used in the next reaction without further purification: MS (ESI) 358.4 (M + H)⁺.

{(S)-1-[3-Hydroxy-5-methyl-1-(pyridine-2-sulfonyl)azepan-4-ylcarbamoyl]-3-methylbutyl}carbamic Acid *tert*-Butyl Ester (23). To a solution of amines **22** (6 g, 16.8 mmol) in CH₂Cl₂ (30 mL) were added 2-pyridinesulfonyl chloride (3 g, 16.9 mmol) and triethylamine (3 mL, 22.5 mmol). The reaction was allowed to stir at room temperature for 16 h, whereupon it was washed with NaHCO₃. The organic layer was dried over sodium sulfate, filtered, concentrated, and purified on a silica gel column (80% EtOAc/hexane) to yield the title compound as a mixture of diastereomers (5.36 g, 48%, two steps): MS (ESI) 499.1 (M + H)⁺.

Benzofuran-2-carboxylic Acid {(S)-3-Methyl-1-[5-methyl-3-hydroxy-1-(pyridine-2-sulfonyl)azepan-4-ylcarbamoyl]butyl}-amide (24). To a solution of sulfonamides **23** (5.36 g, 11.6 mmol) in MeOH (2 mL) was added 4 M HCl/dioxane (25 mL) and the mixture stirred for 2 h at room temperature. The solvent and an excess amount of HCl were removed in vacuo, and the residue was azeotropically dried twice with toluene to yield the primary amine as a hydrochloride salt (5.37 g), which was used in the next reaction without further purification. To a solution of the intermediate amine (0.66 g, 1.26 mmol) in CH₂Cl₂ were added 2-benzofuran carboxylic acid (0.24 g, 1.51 mmol), EDC (0.29 g, 1.51 mmol), HOBT (0.04 g, 0.29 mmol), and Et₃N (1 mL). The reaction mixture was stirred at room temperature for 3 h, whereupon it was washed with an aqueous solution of sodium bicarbonate. The organic layer was dried over sodium sulfate, filtered, and concentrated. The crude product was purified on a silica gel column (80% EtOAc/hexane) to yield the title compound (0.55 g, 62%) as a mixture of diastereomers that was carried on to the next step: MS (ESI) 565.08 (M + N)⁺.

Benzofuran-2-carboxylic Acid {(S)-3-Methyl-1-[5-methyl-3-oxo-1-(pyridine-2-sulfonyl)azepan-4-ylcarbamoyl]butyl}amide (2-5). To a solution of alcohols **24** (0.15 g, 0.27 mmol) in CH₂Cl₂ (2 mL) was added Dess–Martin periodinane (0.17 g, 0.41 mmol). The reaction was stirred at room temperature for 1 h, diluted with CH₂Cl₂, and then washed with aqueous sodium thiosulfate solution, aqueous sodium bicarbonate solution, and brine. The organic layer was washed, dried over sodium sulfate, filtered, concentrated, and purified on a silica gel column (80% EtOAc/hexane) to provide the title compound as a mixture of four diastereomers (0.1 g, 67%). The *cis*-diastereomers **2** and **5** were separated from the *trans*-diastereomers **4** and **3** by HPLC on an Impaq silica gel 10 μm column (4.6 × 250 mm 60 A, 93% CH₂Cl₂/THF, 1.0 mL/min, UV 235 nm). Individual diastereomers from each pair were then separated by HPLC using Chiralcel OD (4.6 × 250 mm, 80% hexane/EtOH, 1 mL/min, UV 235) to provide individual diastereomers as white powders: **2** (32 mg, 21.5%, 8.1 min), **5** (17 mg, 11.4%, 10.9 min) and **4** (7 mg, 4.7%, 8.9 min), **3** (10 mg, 6.7%, 12.9 min). **2**: ¹H NMR (CDCl₃) δ 8.73 (d, *J* = 4.04 Hz, 1H), 8.02–7.93 (m, 2H), 7.68 (d, *J* = 7.58 Hz, 1H), 7.57–7.49 (m, 1H), 7.48–7.42 (m, 1H), 7.33–7.28 (m, 1H), 7.18 (d, *J* = 6.57 Hz, 1H), 7.15 (d, *J* = 8.59 Hz, 1H), 5.32 (dd, *J* = 6.82, 2.78 Hz, 1H), 4.81–4.73 (m, 1H), 3.93 (dd, *J* = 14.91, 1.26 Hz, 1H), 3.81 (d, *J* = 19.20 Hz, 1H), 3.02–2.93 (m, 1H), 2.46 (dd, *J* = 7.33, 3.03 Hz, 1H), 2.39–2.28 (m, 1H), 1.79–1.69 (m, 3H), 1.34–1.24 (m, 3H), 1.05–0.97

(m, 5H), 0.93–0.85 (m, 3H), 0.80 (d, *J* = 7.58 Hz, 2H); MS (ESI) 541.2 (M + H)⁺; analytical HPLC, Impaq silica gel 10 μm column, 4.6 × 250 mm 60 A, 93% CH₂Cl₂/THF, 1.0 mL/min, UV 235 nm, retention time = 9.1 min, >95% purity. Anal. (C₂₇H₃₂N₄O₆S) C, 59.98; H, 5.97; N, 10.36. Found: C, 59.29; H, 5.98; N, 10.14. **5**: ¹H NMR (CDCl₃) δ 8.69 (d, *J* = 4.55 Hz, 1H), 7.99–7.91 (m, 2H), 7.69 (d, *J* = 7.58 Hz, 1H), 7.58–7.50 (m, 2H), 7.45 (td, *J* = 7.83, 1.26 Hz, 1H), 7.34–7.26 (m, 1H), 7.19 (d, *J* = 6.06 Hz, 1H), 7.09 (d, *J* = 8.08 Hz, 1H), 5.30 (dd, *J* = 6.06, 2.78 Hz, 1H), 4.80–4.72 (m, 1H), 4.65 (dd, *J* = 19.33, 1.64 Hz, 1H), 3.93 (s, 1H), 3.78 (d, *J* = 19.20 Hz, 1H), 3.00 (s, 1H), 2.50 (s, 1H), 2.38 (s, 1H), 1.86 (s, 1H), 1.78–1.70 (m, 3H), 1.67 (s, 1H), 1.02 (dd, *J* = 6.32, 2.27 Hz, 6H), 0.84 (d, *J* = 7.33 Hz, 3H); MS (ESI) 541.2 (M + H)⁺; analytical HPLC, Impaq silica gel 10 μm column, 4.6 × 250 mm 60 A, 93% CH₂Cl₂/THF, 1.0 mL/min, UV 235 nm, retention time = 13.4 min, >95% purity. Anal. (C₂₇H₃₂N₄O₆S) C, 59.98; H, 5.97; N, 10.36. Found: C, 59.16; H, 5.93; N, 10.10. **4**: ¹H NMR (CDCl₃) δ 8.70 (d, *J* = 4.29 Hz, 1H), 7.98–7.90 (m, 2H), 7.66 (d, *J* = 7.83 Hz, 1H), 7.55–7.48 (m, 3H), 7.45–7.40 (m, 1H), 7.32–7.26 (m, 1H), 7.15 (d, *J* = 8.34 Hz, 1H), 7.02 (d, *J* = 8.08 Hz, 1H), 5.17–5.11 (m, 1H), 4.82 (td, *J* = 8.65, 5.18 Hz, 1H), 4.59 (dd, *J* = 18.44, 1.52 Hz, 1H), 4.03–3.94 (m, 1H), 3.81 (d, *J* = 18.19 Hz, 1H), 2.93–2.83 (m, 1H), 1.90–1.82 (m, 3H), 1.79–1.70 (m, 3H), 1.14 (d, *J* = 6.82 Hz, 3H), 1.05–0.96 (m, 6H); MS (ESI) 541.2 (M + H)⁺; analytical HPLC, Impaq silica gel 10 μm column, 4.6 × 250 mm 60 A, 93% CH₂Cl₂/THF, 1.0 mL/min, UV 235 nm, retention time = 16.1 min, >95% purity. Anal. (C₂₇H₃₂N₄O₆S) C, 59.98; H, 5.97; N, 10.36. Found: C, 59.87; H, 6.00; N, 9.99. **3**: ¹H NMR (CDCl₃) δ 8.76–8.71 (m, 1H), 8.02–7.93 (m, 2H), 7.68 (d, *J* = 7.33 Hz, 1H), 7.56–7.52 (m, 2H), 7.50 (d, *J* = 1.01 Hz, 1H), 7.44 (td, *J* = 7.83, 1.26 Hz, 1H), 7.34–7.27 (m, 1H), 7.14 (d, *J* = 8.59 Hz, 1H), 6.91 (d, *J* = 8.59 Hz, 1H), 5.20–5.13 (m, 1H), 4.81–4.71 (m, 2H), 4.06–3.96 (m, 1H), 3.88 (d, *J* = 18.44 Hz, 1H), 2.92–2.82 (m, 1H), 1.88–1.83 (m, 2H), 1.81–1.69 (m, 4H), 1.08 (d, *J* = 6.82 Hz, 3H), 1.00 (dd, *J* = 6.06, 3.54 Hz, 6H); MS (ESI) 541.2 (M + H)⁺; analytical HPLC, Impaq silica gel 10 μm column 4.6 × 250 mm 60 A, 93% CH₂Cl₂/THF, 1.0 mL/min, UV 235 nm, retention time = 19.5 min, >95% purity. Anal. (C₂₇H₃₂N₄O₆S) C, 59.98; H, 5.97; N, 10.36. Found: C, 59.02; H, 6.06; N, 10.01.

6-Methylazepanones. Allyl-(2-methylpent-4-enyl)amine (27). To a solution of 2-methylpent-4-enoic acid ethyl ester **25** (7.1 g, 50 mmol) was added dropwise a solution of DIBAL-H (1.0 M in hexanes, 75 mL) at –78 °C over 1 h. After addition, the reaction mixture was stirred at –78 °C for another 1 h. The reaction was quenched with saturated aqueous ammonium chloride (10 mL) and 4% aqueous HCl and then was extracted with EtOAc (3 × 100 mL). The combined organic extracts were dried over MgSO₄, filtered, and concentrated by rotary evaporation. The crude product was used in the next reaction without further purification. 2-Methyl-4-pentenal **26** (3.3 g, 33.7 mmol) was dissolved in CH₂Cl₂ (100 mL). To this solution was added allylamine (2.9 g, 50.5 mmol). Molecular sieves (4 Å, 5 g) were used to absorb the water generated during the reaction. The mixture was stirred at room temperature overnight. The reaction mixture was concentrated by rotary evaporation and the crude product was used in the next reaction without further purification. Allyl-(2-methylpent-4-enylidene)amine (3.2 g, 23.4 mmol) was diluted in 50 mL of MeOH. To the above solution was added NaBH₄ (1.0 g, 26.3 mmol) at 0 °C. After addition, the mixture was stirred at room temperature for 5 h. The reaction mixture was concentrated and the residue was partitioned between EtOAc and 20% aqueous NaOH. The organic layer was dried over Na₂SO₄, filtered, and concentrated by rotary evaporation to give the title compound (1.5 g, 48%): ¹H NMR (CDCl₃) δ 5.93–5.68 (m, 2H), 5.18–4.92 (m, 4H), 3.21 (d, *J* = 5.2 Hz, 2H), 2.60–2.40 (m, 2H), 1.97–1.65 (m, 2H), 0.92 (d, *J* = 7.6 Hz, 3H).

Pyridine-2-sulfonic Acid Allyl(2-methylpent-4-enyl)amide (28). Allyl(2-methylpent-4-enyl)amine **27** (1.0 g, 7.2 mmol) and 4-methylmorpholine (1.7 g, 17.2 mmol) were mixed in 30 mL of CH₂Cl₂. 2-Pyridinesulfonyl chloride (1.53 g, 8.6 mmol) was added slowly to the solution while it was cooled in an ice–water bath. After addition, the reaction mixture was stirred at room temperature

overnight. The reaction mixture was washed with 10% aqueous NaHCO₃ and brine and then was purified by column chromatography to give the title compound as a colorless oil (1.2 g, 60%): ¹H NMR (CDCl₃) δ 8.72–8.69 (m, 1H), 8.00–7.75 (m, 2H), 7.49–7.47 (m, 1H), 5.80–5.60 (m, 2H), 5.15–4.92 (m, 4H), 4.00–3.90 (m, 2H), 3.20–3.06 (m, 2H), 2.19–2.12 (m, 1H), 1.91–1.85 (m, 2H), 0.89 (d, *J* = 6.4 Hz, 3H); MS (ESI) 281.2 (M + H)⁺.

3-Methyl-1-(pyridine-2-sulfonyl)-2,3,4,7-tetrahydro-1H-azepine (29). Pyridine-2-sulfonic acid allyl(2-methylpent-4-enyl)-amide **28** (1.2 g, 4.3 mmol) was dissolved in CH₂Cl₂ (100 mL). After carefully degassing with argon, bis(tricyclohexylphosphine)-benzylidineruthenium(IV) dichloride (0.35 g, 0.43 mmol) was added under argon. The mixture was then refluxed for 2 h before the reaction mixture was concentrated by rotary evaporation. The product was purified by column chromatography (5%–20% EtOAc/hexane) to give the title compound (0.9 g, 83% yield): ¹H NMR (CDCl₃) δ 8.70 (d, *J* = 4.4 Hz, 1H), 8.00–7.75 (m, 2H), 7.52–7.49 (m, 1H), 5.79–5.60 (m, 2H), 4.00 (d, *J* = 4.8 Hz, 2H), 3.65 (dd, *J* = 12.8, 4.0 Hz, 1H), 3.22 (dd, *J* = 13.3, 9.1 Hz, 1H), 2.30–2.05 (m, 3H), 0.96 (d, *J* = 6.4 Hz, 3H); MS (ESI) 253.2 (M + H)⁺.

5-Methyl-3-(pyridine-2-sulfonyl)-8-oxa-3-azabicyclo[5.1.0]octane (30 and 31). To a solution of 3-methyl-1-(pyridine-2-sulfonyl)-2,3,4,7-tetrahydro-1H-azepine **29** (1.3 g, 5.16 mmol) in CH₂Cl₂ (50 mL) were added NaHCO₃ (1.3 g, 15.5 mmol) and *m*CPBA (2.67 g, 15.5 mmol) in portions. The reaction was stirred at room temperature for 4 h before working up by washing with 15% aqueous NaOH, saturated aqueous K₂CO₃ and brine, followed by drying over Na₂SO₄. After filtration, the organic solution was concentrated by rotary evaporation, and the two isomers were separated on column chromatography (30%–40% EtOAc/hexane). **30** (*cis*-isomer, 230 mg, 17%), **31** (*trans*-isomer, 200 mg, 14%), and a mixture of **30** and **31** (570 mg, 46%) were used in next steps, carried on separately. **30**: ¹H NMR (CDCl₃) δ 8.70 (d, *J* = 4.8 Hz, 1H), 8.00–7.75 (m, 2H), 7.54–7.48 (m, 1H), 4.41–4.37 (m, 1H), 3.93–3.90 (m, 1H), 3.34–2.00 (m, 6H), 1.45–1.35 (m, 1H), 0.88 (d, *J* = 7.0 Hz, 3H); MS (ESI) 269.0 (M + H)⁺. **31**: ¹H NMR (CDCl₃) δ 8.68–8.66 (m, 1H), 7.98–7.87 (m, 2H), 7.49–7.46 (m, 1H), 4.06–3.98 (m, 1H), 3.60–3.55 (m, 1H), 3.35–3.22 (m, 2H), 3.14–3.06 (m, 2H), 2.10–1.90 (m, 3H), 1.02 (d, *J* = 6.6 Hz, 3H); MS (ESI) 269.2 (M + H)⁺.

4-Azido-5-methyl-1-(pyridine-2-sulfonyl)azepan-3-ol (32). 5-Methyl-3-(pyridine-2-sulfonyl)-8-oxa-3-azabicyclo[5.1.0]octane **30** (230 mg, 0.86 mmol) was dissolved in 8 mL of MeOH and 2 mL of H₂O. NaN₃ (170 mg, 2.6 mmol) and ammonium chloride (140 mg, 2.6 mmol) were added to the above solution. The reaction mixture was refluxed overnight. After the removal of MeOH, the residue was diluted in EtOAc and washed with 10% aqueous NaHCO₃ and brine. The product was purified by column chromatography (1% MeOH/CH₂Cl₂) to give the title compound (170 mg, 64%): ¹H NMR (CDCl₃) δ 8.69 (d, *J* = 4.8 Hz, 1H), 8.04–7.94 (m, 2H), 7.56–7.53 (m, 1H), 4.00–2.95 (m, 7H), 2.23–2.14 (m, 1H), 1.90–1.74 (m, 2H), 0.98 (d, *J* = 6.9 Hz, 3H); MS (ESI) 312.2 (M + H)⁺.

4-Azido-5-methyl-1-(pyridine-2-sulfonyl)azepan-3-ol (33). 5-Methyl-3-(pyridine-2-sulfonyl)-8-oxa-3-azabicyclo[5.1.0]octane **31** (700 mg, 2.6 mmol) was dissolved in 16 mL of MeOH and 4 mL of H₂O. NaN₃ (510 mg, 7.8 mmol) and ammonium chloride (420 mg, 7.8 mmol) were added to the solution. The resulting mixture was refluxed overnight. After evaporation of MeOH, the residue was diluted in EtOAc and washed with 10% aqueous NaHCO₃ and brine. The product was purified by column chromatography (1% MeOH/CH₂Cl₂) to give the title compound (530 mg, 66%): ¹H NMR δ 8.69–8.67 (m, 1H), 8.05–7.70 (m, 2H), 7.53–7.50 (m, 1H), 3.90–3.45 (m, 5H), 2.88–2.80 (m, 1H), 2.08–1.50 (m, 4H), 0.95 (d, *J* = 6.7 Hz, 3H); MS (ESI) 312.2 (M + H)⁺.

4-Amino-6-methyl-1-(pyridine-2-sulfonyl)azepan-3-ol (34). 4-Azido-6-methyl-1-(pyridine-2-sulfonyl)azepan-3-ol (**32**, 0.48 g, 1.54 mmol) was dissolved in THF (50 mL) and H₂O (0.2 mL). Triphenylphosphine (0.61 g, 2.32 mmol) was added to this solution. The reaction mixture was stirred at 45 °C overnight. THF was

evaporated and the remaining material was azeotroped twice with toluene (100 mL). The resulting thick oil was dissolved in MeOH and treated with HCl in ether to adjust pH to acidic. Additional ether was added and the solution turned cloudy to give the title compound as a white precipitate that was collected by filtration (0.27 g, 71%): ¹H NMR (CD₃OD) δ 8.72 (d, *J* = 4.8 Hz, 1H), 8.14–7.99 (m, 2H), 7.70–7.66 (m, 1H), 3.85–3.69 (m, 2H), 3.38–3.22 (m, 3H), 3.10–3.04 (m, 2H), 2.08–2.00 (m, 1H), 1.82–1.66 (m, 2H), 1.02 (d, *J* = 6.8 Hz, 3H); MS (ESI) 286.0 (M + H)⁺.

4-Amino-6-methyl-1-(pyridine-2-sulfonyl)azepan-3-ol (35). 4-Azido-6-methyl-1-(pyridine-2-sulfonyl)azepan-3-ol **33** (0.48 g, 1.54 mmol) was dissolved in THF (50 mL) and H₂O (0.2 mL). Triphenylphosphine (0.61 g, 2.32 mmol) was added to this solution. The reaction mixture was stirred at 45 °C overnight. THF was evaporated and azeotroped by toluene (2 × 100 mL). The resulting thick oil was dissolved in MeOH and treated with HCl in ether to adjust pH to acidic. Additional ether was added and the solution turned cloudy to give the title compound as a white precipitate that was collected by filtration (0.27 g, 71%): ¹H NMR (CDCl₃) δ 8.73 (d, *J* = 4.8 Hz, 1H), 8.13–7.99 (m, 2H), 7.70–7.66 (m, 1H), 3.84–3.80 (m, 1H), 3.74–3.66 (m, 1H), 3.38–3.21 (m, 3H), 3.10–3.06 (m, 2H), 2.05 (brs, 1H), 1.85–1.66 (m, 2H), 1.02 (d, *J* = 6.7 Hz, 3H); MS (ESI) 286.0 (M + H)⁺.

{(S)-1-[3-Hydroxy-6-methyl-1-(pyridine-2-sulfonyl)azepan-4-ylcarbamoyl]-3-methylbutyl}carbamoyl tert-Butyl Ester (36a, 36b). 4-Amino-6-methyl-1-(pyridine-2-sulfonyl)azepan-3-ol **34** HCl salt (0.11 g, 0.59 mmol) was dissolved in 5 mL of DMF. To this solution were added Boc-L-leucine (0.22 g, 0.88 mmol), HBTU (0.34 g, 0.90 mmol), and *N*-methylmorpholine (0.24 g, 2.4 mmol). The reaction mixture was stirred at room temperature overnight. DMF was removed under high vacuum. The residue was diluted in EtOAc and washed with H₂O, 10% aqueous NaHCO₃, and brine. Purification by column chromatography (50% EtOAc/hexane) gave the title compound as a mixture of diastereomers (0.2 g, 68%): ¹H NMR (CDCl₃) δ 8.75 (d, *J* = 4.4 Hz, 1H), 8.0–7.75 (m, 2H), 7.56–7.50 (m, 1H), 5.10–5.00 (m, 1H), 4.15–2.90 (m, 10H), 2.10–1.48 (m, 14H), 1.05–1.00 (m, 9H); MS (ESI) 499.1 (M + H)⁺.

{(S)-1-[3-Hydroxy-6-methyl-1-(pyridine-2-sulfonyl)azepan-4-ylcarbamoyl]-3-methylbutyl}carbamoyl tert-Butyl Ester (37a, 37b). 4-Amino-6-methyl-1-(pyridine-2-sulfonyl)azepan-3-ol **35** HCl salt (0.27 g, 0.76 mmol) was dissolved in 5 mL of DMF. To this solution were added Boc-L-leucine (0.23 g, 0.91 mmol), HBTU (0.35 g, 0.91 mmol), and *N*-methylmorpholine (0.39 g, 3.0 mmol). The reaction mixture was stirred at room temperature overnight. DMF was removed under high vacuum. The residue was diluted in EtOAc and washed with H₂O, 10% NaHCO₃, and brine. Purification by column chromatography (50% EtOAc/hexane) gave the title compound as a mixture of diastereomers (0.35 g, 92%): ¹H NMR (CDCl₃) δ 8.70 (d, *J* = 4.0 Hz, 1H), 7.99–7.92 (m, 2H), 7.55–7.48 (m, 1H), 6.46–6.42 (m, 1H), 4.60 (brs, 1H), 4.11–4.02 (m, 1H), 3.88–3.38 (m, 5H), 3.02–2.95 (m, 3H), 2.05 (brs, 1H), 1.68–1.63 (m, 4H), 1.45 (s, 9H), 0.97–0.93 (m, 9H); MS (ESI) 499.1 (M + H)⁺.

Benzofuran-2-carboxylic Acid {(S)-1-[3-Hydroxy-6-methyl-1-(pyridine-2-sulfonyl)azepan-4-ylcarbamoyl]-3-methylbutyl}-amide (38a, 38b). {(S)-1-[3-Hydroxy-6-methyl-1-(pyridine-2-sulfonyl)azepan-4-ylcarbamoyl]-3-methylbutyl}carbamoyl tert-butyl ester **36** (0.18 g, 0.36 mmol) was dissolved in 4 M HCl in dioxane (2.8 mL, 11.2 mmol). The mixture was stirred at room temperature for 2 h before solvents and an excess amount of HCl were removed by rotary evaporation. The resulting white solid was dissolved in 5 mL of DMF. To the solution were added benzofuran-2-carboxylic acid (0.074 g, 0.46 mmol), HBTU (0.174 g, 0.46 mmol), and *N*-methylmorpholine (0.15 g, 1.52 mmol). The reaction mixture was stirred at room temperature overnight. DMF was then removed and the residue was dissolved in EtOAc (50 mL) and washed with 10% aqueous NaHCO₃ (50 mL × 2) and brine (50 mL). The combined organics were concentrated by rotary evaporation. Purification by column chromatography (70% EtOAc/hexane) gave the title compound as a mixture of diastereomers (0.15 g, 92%),

two steps): $^1\text{H NMR}$ (CDCl_3) δ 8.74–8.65 (m, 1H), 7.93–7.87 (m, 2H), 7.64–7.23 (m, 8H), 4.77–4.73 (m, 1H), 4.18–3.19 (m, 5H), 3.01–2.80 (m, 1H), 1.90–1.44 (m, 5H), 0.99–0.94 (m, 8H), 0.88–0.84 (m, 3H); MS (ESI) 543.2 ($\text{M} + \text{H}$) $^+$.

Benzofuran-2-carboxylic Acid {(S)-1-[3-Hydroxy-6-methyl-1-(pyridine-2-sulfonyl)azepan-4-ylcarbamoyl]-3-methylbutyl}-amide (39). {(S)-1-[3-Hydroxy-6-methyl-1-(pyridine-2-sulfonyl)azepan-4-ylcarbamoyl]-3-methylbutyl}carbamic acid *tert*-butyl ester **37a** and **37b** (0.35 g, 0.70 mmol) were dissolved in 4 M HCl in dioxane (3.5 mL, 14 mmol). The reaction mixture was stirred at room temperature for 2 h before solvents and an excess amount of HCl were removed by rotary evaporation. The resulting white solid was dissolved in 5 mL of DMF. To the solution were added benzofuran-2-carboxylic acid (0.15 g, 0.91 mmol), HBTU (0.35 g, 0.91 mmol), and *N*-methylmorpholine (0.3 g, 3.0 mmol). The mixture was stirred at room temperature overnight. DMF was then removed and the residue was dissolved in EtOAc (50 mL) and washed with 10% aqueous NaHCO_3 (50 mL \times 2) and brine (50 mL). The combined organics were concentrated by rotary evaporation. Purification by column chromatography (70% EtOAc/hexane) gave the title compounds (0.32 g, 84%, two steps): $^1\text{H NMR}$ (CDCl_3) δ 8.69–8.66 (m, 1H), 8.02–7.86 (m, 2H), 7.68–7.03 (m, 8H), 4.75–4.68 (m, 1H), 3.79–3.38 (m, 7H), 3.10–2.87 (m, 1H), 1.96–1.64 (m, 5H), 1.06–0.86 (m, 9H); MS (ESI) 543.2 ($\text{M} + \text{H}$) $^+$.

Benzofuran-2-carboxylic Acid {(S)-3-Methyl-1-[(4S,6S)-6-methyl-3-oxo-1-(pyridine-2-sulfonyl)azepan-4-ylcarbamoyl]butyl}-amide (7) and Benzofuran-2-carboxylic Acid {(S)-3-Methyl-1-[(4R,6R)-6-methyl-3-oxo-1-(pyridine-2-sulfonyl)azepan-4-ylcarbamoyl]butyl}amide (8). To a solution of benzofuran-2-carboxylic acid {(S)-1-[3-hydroxy-6-methyl-1-(pyridine-2-sulfonyl)azepan-4-ylcarbamoyl]-3-methylbutyl}amide **38a** and **38b** (0.15 g, 0.28 mmol) in 5 mL of CH_2Cl_2 was added Dess–Martin periodinane (0.176 g, 0.42 mmol) at room temperature. The solution was stirred for 2 h. An additional 50 mL of CH_2Cl_2 was added and then the mixture was washed with 10% aqueous NaHCO_3 and brine. Purification by column chromatography (50% EtOAc/hexane) gave the title compounds (0.13 g, 87%). The diastereomers were separated by HPLC using a Whelk-O (*R,R*) chiral prep column (21.1 \times 250 mm, 50% EtOH/hexane, 20 mL/min, UV 235) to provide individual diastereomers as white powders: **7** (45 mg, 30%, 13.9 min), **8** (40 mg, 27%, 16.9 min). **7**: $^1\text{H NMR}$ (CDCl_3) δ 8.69 (d, $J = 4.0$ Hz, 1H), 7.94–7.90 (m, 2H), 7.65 (d, $J = 8.0$ Hz, 1H), 7.52–7.02 (m, 7H), 5.28–5.02 (m, 1H), 4.78–4.60 (m, 1H), 3.88–3.50 (m, 2H), 3.31–3.19 (m, 1H), 3.02–2.97 (m, 1H), 2.10–1.45 (m, 6H), 1.20 (d, $J = 6.6$ Hz, 3H), 0.98 (d, $J = 4.4$ Hz, 6H); MS (ESI) 541.2 ($\text{M} + \text{H}$) $^+$; analytical HPLC, Whelk-O (*R,R*) 5 μm , 4.6 \times 250 mm, 50% EtOH/hexane, 1.0 mL/min, UV 215 nm, retention time = 12.9 min, >95% purity. Anal. ($\text{C}_{27}\text{H}_{32}\text{N}_4\text{O}_6\text{S}$) C, 59.98; H, 5.97; N, 10.36. Found: C, 60.01; H, 5.94; N, 10.11. **8**: $^1\text{H NMR}$ (CDCl_3) δ 8.64 (d, $J = 4.0$ Hz, 1H), 7.95–7.88 (m, 2H), 7.65 (d, $J = 8.0$ Hz, 1H), 7.53–7.38 (m, 3H), 7.30–7.25 (m, 2H), 7.08–7.04 (m, 2H), 5.20–5.15 (m, 1H), 4.78–4.70 (m, 1H), 4.45 (d, $J = 12$ Hz, 1H), 3.86 (d, $J = 12.0$ Hz, 1H), 3.59–3.50 (m, 1H), 3.08–3.02 (m, 1H), 2.10–2.00 (m, 2H), 1.87–1.61 (m, 4H), 1.20 (d, $J = 6.2$ Hz, 3H), 0.99 (d, $J = 4.0$ Hz, 6H); MS (ESI) 541.2 ($\text{M} + \text{H}$) $^+$; analytical HPLC, Whelk-O (*R,R*) 5 μm , 4.6 \times 250 mm, 50% EtOH/hexane, 1.0 mL/min, UV 215 nm, retention time = 15.9 min; > 95% purity.

Benzofuran-2-carboxylic Acid {(S)-3-Methyl-1-[(4S,6S)-6-methyl-3-oxo-1-(pyridine-2-sulfonyl)azepan-4-ylcarbamoyl]butyl}-amide (9) and Benzofuran-2-carboxylic Acid {(S)-3-Methyl-1-[(4R,6R)-6-methyl-3-oxo-1-(pyridine-2-sulfonyl)azepan-4-ylcarbamoyl]butyl}amide (6). To a solution of benzofuran-2-carboxylic acid {(S)-1-[3-hydroxy-6-methyl-1-(pyridine-2-sulfonyl)azepan-4-ylcarbamoyl]-3-methylbutyl}amide **38** (0.32 g, 0.89 mmol) in 5 mL of CH_2Cl_2 was added Dess–Martin periodinane (0.38 g, 0.89 mmol) at room temperature. The solution was stirred for 2 h. An additional 50 mL of CH_2Cl_2 was added and then the mixture was washed with 10% aqueous NaHCO_3 and brine. Purification by column chromatography (50% EtOAc/hexane) gave the title

compound (0.25 g, 78%). The diastereomers were separated by HPLC using a Whelk-O (*R,R*) chiral prep column, 21.1 \times 250 mm, 40% EtOH/hexane, 20 mL/min, UV 235 to provide individual diastereomers as white powders: **9** (100 mg, 31%, 14.2 min), **6** (100 mg, 31%, 16.7 min). **9**: $^1\text{H NMR}$ (CDCl_3) δ 8.69 (d, $J = 4.8$ Hz, 1H), 7.98–7.91 (m, 2H), 7.66 (d, $J = 7.6$ Hz, 1H), 7.54–7.01 (m, 7H), 5.23–5.19 (m, 1H), 4.82–4.73 (m, 2H), 3.98–3.96 (m, 1H), 3.83 (d, $J = 4.8$ Hz, 1H), 2.36–2.31 (m, 1H), 2.17–2.04 (m, 3H), 1.74–1.73 (m, 2H), 1.25–1.14 (m, 1H), 1.00 (d, $J = 4.4$ Hz, 6H), 0.87 (d, $J = 6.0$ Hz, 3H); MS (ESI) 541.2 ($\text{M} + \text{H}$) $^+$; analytical HPLC, Whelk-O (*R,R*) 5 μm , 4.6 \times 250 mm, 40% EtOH/hexane, 1.0 mL/min, UV 215 nm, retention time = 12.0 min, >95% purity. Anal. ($\text{C}_{27}\text{H}_{32}\text{N}_4\text{O}_6\text{S}$) C, 59.98; H, 5.97; N, 10.36. Found: C, 59.72; H, 5.52; N, 10.21. **6**: δ 8.64 (d, $J = 5.2$ Hz, 1H), 7.93–7.87 (m, 2H), 7.63 (d, $J = 8.0$ Hz, 1H), 7.49–7.37 (m, 4H), 7.28–7.17 (m, 3H), 5.21–5.17 (m, 1H), 4.80–4.70 (m, 2H), 3.97–3.94 (m, 1H), 3.80–3.69 (m, 1H), 2.36–2.30 (m, 1H), 2.15–2.11 (m, 3H), 1.83–1.70 (m, 2H), 1.25–1.16 (m, 1H), 0.98 (d, $J = 5.2$ Hz, 6H), 0.89 (d, $J = 6.0$ Hz, 3H); MS (ESI) 541.2 ($\text{M} + \text{H}$) $^+$; analytical HPLC, Whelk-O (*R,R*) 5 μm , 4.6 \times 250 mm, 40% EtOH/hexane, 1.0 mL/min, UV 215 nm, retention time = 13.9 min, >95% purity.

7-Methylazepanones. Allyl-(1-methylpent-4-enyl)amine (41). Hex-5-en-2-one **40** (9.8 g, 11.6 mL, 100 mmol) was added to a stirred solution of allylamine (8.55 mmol, 11.25 mL, 150 mmol), 4 Å molecular sieves (52 g), and *p*-TsOH (10 mg) in CH_2Cl_2 (200 mL) and the mixture was stirred overnight and then filtered. The reaction mixture was concentrated by rotary evaporation and was used in the next reaction without further purification (13 g, 95%). To a stirred solution of allyl(1-methylpent-4-enylidene)amine (6.5 g, 47 mmol) in MeOH (100 mL) at 0 °C was added sodium borohydride (2.7 g, 71 mmol) portionwise. The reaction mixture was stirred for 30 min and then warmed to room temperature. Approximately 90 mL of MeOH was removed from the reaction mixture by rotary evaporation. The resultant reaction mixture was diluted with ether (200 mL) and then washed with water and brine. The combined organics were dried over MgSO_4 , filtered, and concentrated by rotary evaporation to give a pale yellow liquid that was used in the next reaction without further purification (5.2 g, 80%).

Allyl(1-methylpent-4-enyl)carbamic Acid Benzyl Ester (42). Carbobenzyloxy chloride (9.56 g, 8 mL, 55.6 mmol) was added dropwise to a stirred solution of allyl(1-methylpent-4-enyl)amine **41** (7 g, 50 mmol) and triethylamine (5.8 g, 8.0 mL, 57.5 mmol) in CH_2Cl_2 (100 mL) at 0 °C. The reaction mixture was warmed to room temperature and was stirred for 2 h. The reaction mixture was diluted with CH_2Cl_2 (100 mL), followed by washing with water and brine. The combined organics were dried over MgSO_4 , filtered, concentrated by rotary evaporation and then were purified by column chromatography (silica gel, 4% EtOAc/hexane) to give the title compound (8.9 g, 65%): MS (ESI) 274.2 ($\text{M} + \text{H}$) $^+$.

2-Methyl-2,3,4,7-tetrahydroazepine-1-carboxylic Acid Benzyl Ester (43). Allyl(1-methylpent-4-enyl)carbamic acid benzyl ester **42** (1.04 g, 3.8 mmol) was dissolved in CH_2Cl_2 (10 mL) and a stream of argon gas was bubbled into the reaction mixture for 10 min. Bis(tricyclohexylphosphine)benzylidineruthenium(IV) dichloride (Strem Chemicals, 22 mg, 0.027 mmol) was added and the reaction mixture was refluxed for 2 h. Additional bis(tricyclohexylphosphine)benzylidineruthenium(IV) dichloride (11 mg, 0.014 mmol) was added and the reaction mixture was refluxed for an additional 1.5 h. The reaction mixture was cooled to room temperature under argon overnight, concentrated by rotary evaporation, and then purified by column chromatography (silica gel, 5% EtOAc/hexane) to give the title compound (0.83 g, 89%): $^1\text{H NMR}$ (CDCl_3) δ 7.35–7.20 (m, 5H), 5.65–5.60 (1H, m), 5.15–5.12 (m, 2H), 4.45–4.05 (m, 2H), 3.63–5.57 (m, 1H), 2.25–2.10 (m, 2H), 1.90–1.60 (m, 2H), 1.15–1.12 (m, 3H); MS (ESI) 246.2 ($\text{M} + \text{H}$) $^+$.

4-Methyl-8-oxa-3-azabicyclo[5.1.0]octane-3-carboxylic Acid Benzyl Ester (44 and 45). *m*CPBA (1.05 g, 57–86% pure) was added to a solution of 2-methyl-2,3,4,7-tetrahydroazepine-1-carboxylic acid benzyl ester **43** (0.83 g, 3.39 mmol) in CH_2Cl_2 (45

mL) at 0 °C. The reaction mixture was stirred for 0.5 h and then was warmed to room temperature. Additional *m*-chloroperbenzoic acid (0.3 g, 57–86% pure) was added and the reaction mixture was stirred for 2 h at room temperature. The reaction mixture was concentrated by rotary evaporation, 80 mL of 10% EtOAc/hexane was added, and the reaction mixture was filtered. The filtrate was concentrated by rotary evaporation and then was purified by column chromatography (silica gel, 20% EtOAc/hexane) to give *cis*-4-methyl-8-oxa-3-azabicyclo[5.1.0]octane-3-carboxylic acid benzyl ester **44** (0.44 g, 50%) [¹H NMR (CDCl₃) δ 7.42–7.22 (m, 5H), 5.13 (brs, 2H), 4.50–4.15 (m, 2H), 3.28 (brd, *J* = 16.0 Hz, 1H), 3.12–2.95 (m, 1H), 2.15–1.70 (m, 2H), 1.41–1.38 (m, 2H), 1.06 (brd, *J* = 6.6 Hz, 3H); MS (ESI) 262.0 (M + H)⁺] and *trans*-4-methyl-8-oxa-3-azabicyclo[5.1.0]octane-3-carboxylic acid benzyl ester **45** (0.15 g, 17%) [¹H NMR (CDCl₃) δ 7.37–7.30 (m, 5H), 5.19–5.11 (m, 2H), 4.31–4.05 (m, 2H), 3.44–3.25 (m, 1H), 3.07–2.94 (m, 2H), 2.28–2.16 (m, 1H), 1.90–1.70 (m, 1H), 1.55–1.32 (m, 2H), 1.04–1.01 (m, 3H); MS (ESI) 262.0 (M + H)⁺].

trans-5-Azido-6-hydroxy-2-methylazepane-1-carboxylic Acid Benzyl Ester (46). Sodium azide (0.56 g, 8.6 mmol) was added to a solution of *trans*-4-methyl-8-oxa-3-azabicyclo[5.1.0]octane-3-carboxylic acid benzyl ester **44** (0.75 g, 2.87 mmol) and ammonium chloride (0.46 g, 8.6 mmol) in MeOH (5 mL) and H₂O (0.5 mL) and then was refluxed for 6 h. The reaction mixture was concentrated by rotary evaporation and then was diluted with water (5 mL) and extracted with EtOAc (10 mL). The organic layer was then washed with water and brine, dried over MgSO₄, filtered, concentrated by rotary evaporation, and purified by column chromatography (silica gel, 20% EtOAc/hexane) to yield the title compound (0.7 g, 80%): ¹H NMR (CDCl₃) δ 7.39–7.30 (m, 5H), 5.15 (s, 2H), 4.10–3.67 (m, 5H), 3.10 (d, *J* = 16.0 Hz, 1H), 1.90–1.80 (m, 2H), 1.80–1.53 (m, 2H), 1.09 (d, *J* = 6.6 Hz, 3H); MS (ESI) 305.2 (M + H)⁺.

5-Azido-6-hydroxy-2-methylazepane-1-carboxylic Acid Benzyl Ester (47). Sodium azide (1.8 g, 27.7 mmol) was added to a solution of *cis*-4-methyl-8-oxa-3-azabicyclo[5.1.0]octane-3-carboxylic acid benzyl ester **45** (2.4 g, 9.2 mmol) and ammonium chloride (1.48 g, 27.7 mmol) in MeOH (16 mL) and H₂O (1.6 mL) and then was refluxed overnight. The reaction mixture was concentrated by rotary evaporation and then was diluted with water (5 mL) and extracted with EtOAc. The organic layer was then washed with water and brine, dried over MgSO₄, filtered, and concentrated by rotary evaporation. The crude product was stirred with ether and filtered to give the title compound **47** (1.4 g, 50%). The mother liquors were concentrated by rotary evaporation and the residue was purified by chromatography (silica gel, 20% EtOAc/hexane) to yield the title compound, **47** (0.36 g, 13%; combined yield = 1.76 g, 63%): ¹H NMR (CDCl₃) (shown as two rotamers): δ 7.40–7.28 (m, 5H), 5.20–5.12 (m, 2H), 4.20–3.98 (m, 1H), 3.90–3.75 (m, 1H), 3.65–3.43 (m, 1H), 3.23–3.10 (m, 1H), 2.87 and 2.83 (d each, *J* = 10.8 Hz, 1H), 2.55 and 2.29 (d each, *J* = 2.8 Hz, 1H), 2.10–1.90 (m, 2H), 1.50–1.25 (m, 2H), 1.10 (m, 3H); MS (ESI) 305.2 (M + H)⁺; and the regioisomer, **48** (0.5 g, 18%): NMR (CDCl₃) δ 7.39–7.27 (m, 5H), 5.30–5.05 (m, 2H), 4.16–3.90 (m, 3H), 3.59–3.50 (m, 1H), 3.35 (d, *J* = 15.3 Hz, 1H), 1.88–1.60 (m, 4H), 1.13–1.08 (m, 3H); MS (ESI) 305.2 (M + H)⁺.

5-Amino-6-hydroxy-2-methylazepane-1-carboxylic Acid Benzyl Ester (49). Triphenylphosphine (1.94 g, 7.4 mmol) was added to a solution of 5-azido-6-hydroxy-2-methylazepane-1-carboxylic acid benzyl ester **46** (1.5 g, 4.93 mmol) in THF (185 mL) and H₂O (0.7 mL) and then was heated to 45 °C overnight. The solvent was removed, the residue was azeotroped twice with toluene, and the resulting oil was dissolved in MeOH and HCl in Et₂O. Additional Et₂O was added and the resulting salt was collected following filtration and was used in the next reaction without further purification (1.4 g, 90%).

5-Amino-6-hydroxy-2-methylazepane-1-carboxylic Acid Benzyl Ester (50). Triphenylphosphine (2.13 g, 8.14 mmol) was added to a solution of 5-azido-6-hydroxy-2-methylazepane-1-carboxylic acid benzyl ester **47** (1.6 g, 5.43 mmol) in THF (185 mL) and H₂O (0.7 mL) and then was heated to 45 °C overnight. The reaction

mixture was then azeotroped twice with toluene by rotary evaporation. The resulting oil was dissolved in MeOH and HCl in Et₂O and the resulting salt was collected following filtration and was used in the next reaction without further purification (1.7 g, 100%).

5-((S)-2-tert-Butoxycarbonylamino-4-methylpentanoylamino)-6-hydroxy-2-methylazepane-1-carboxylic Acid Benzyl Ester (51a, 51b). EDC (0.33 g, 1.73 mmol) was added to a solution of Boc-L-leucine hydrate (0.43 g, 1.7 mmol), diisopropylethylamine (0.22 g, 0.3 mL, 1.7 mmol), HOBT (0.25 g, 1.85 mmol), and 5-amino-6-hydroxy-2-methylazepane-1-carboxylic acid benzyl ester **49** (0.5 g, 1.6 mmol) in DMF (10 mL). The reaction mixture was stirred overnight at room temperature and then was diluted with EtOAc (100 mL), washed with H₂O (3 × 50 mL) and brine (50 mL), dried over magnesium sulfate, filtered, concentrated by rotary evaporation, and purified by column chromatography (silica gel, 50% EtOAc/hexane) to yield the title compound as a mixture of diastereomers (0.78 g, 100%): ¹H NMR (CDCl₃) δ 7.40–7.29 (m, 5H), 6.75 (brd, 1H), 5.18–5.11 (m, 2H), 5.05 (brs, 1H), 4.15–3.72 (m, 5H), 3.06 (d, *J* = 16.0 Hz, 1H), 1.90–1.40 (m, 7H), 1.40 (s, 9H); 1.12–1.05 (m, 3H), 0.97–0.87 (m, 6H); MS (ESI) 492.0 (M + H)⁺.

5-((S)-2-tert-Butoxycarbonylamino-4-methylpentanoylamino)-6-hydroxy-2-methylazepane-1-carboxylic Acid Benzyl Ester (52a, 52b). EDC (1.0 g, 5.2 mmol) was added to a solution of Boc-L-leucine hydrate (1.31 g, 5.26 mmol), diisopropylethylamine (0.74 g, 1.0 mL, 5.75 mmol), HOBT (0.77 g, 5.69 mmol), and 5-amino-6-hydroxy-2-methylazepane-1-carboxylic acid benzyl ester **50** (1.5 g, 4.77 mmol) in DMF (30 mL). The reaction mixture was stirred overnight at room temperature and then was diluted with EtOAc (100 mL), washed with H₂O (3 × 50 mL) and brine (50 mL), dried over magnesium sulfate, filtered, concentrated by rotary evaporation, and purified by column chromatography (silica gel, 60% EtOAc/hexane) to yield the title compound (2.1 g, 90%): ¹H NMR (CDCl₃) δ 7.45–7.31 (m, 5H), 6.72–6.49 (m, 1H), 5.20–4.93 (m, 2H), 4.12–3.45 (m, 5H), 2.98–2.85 (m, 1H), 2.02–1.30 (m, 7H), 1.40 (s, 9H), 1.12–1.07 (m, 3H), 0.98–0.90 (m, 6H).

[(S)-1-(3-Hydroxy-7-methylazepan-4-ylcarbonyl)-3-methylbutyl]carbamic Acid tert-Butyl Ester (53a, 53b). 5-((S)-2-tert-Butoxycarbonylamino-4-methylpentanoylamino)-6-hydroxy-2-methylazepane-1-carboxylic acid benzyl ester (**51a, 51b**) (0.77 g, 1.57 mmol) was dissolved in EtOAc (27.5 mL) and MeOH (5.5 mL). Ten percent Pd/C (0.39 g) was added and the reaction mixture was stirred overnight under a balloon filled with hydrogen gas. The reaction mixture was filtered through Celite, concentrated by rotary evaporation, and used in the next reaction without further purification (0.56 g, 99%): MS (ESI) 358.1 (M + H)⁺.

[(S)-1-(3-Hydroxy-7-methylazepan-4-ylcarbonyl)-3-methylbutyl]carbamic Acid tert-Butyl Ester (54a, 54b). 5-((S)-2-tert-Butoxycarbonylamino-4-methylpentanoylamino)-6-hydroxy-2-methylazepane-1-carboxylic acid benzyl ester (**52a, 52b**) (2.1 g, 4.28 mmol) was dissolved in EtOAc (75 mL) and MeOH (15 mL). 10% Pd/C (1.05 g) was added and the reaction mixture was stirred overnight under a balloon filled with hydrogen gas. The reaction mixture was filtered through Celite, concentrated by rotary evaporation, and used in the next reaction without further purification (1.53 g, 99%): MS (ESI) 358.2 (M + H)⁺.

[(S)-1-Benzenesulfonyl-3-hydroxy-7-methylazepan-4-ylcarbonyl]-3-methylbutyl]carbamic Acid tert-Butyl Ester (55a, 55b). 2-Pyridinesulfonyl chloride (0.6 g, 3.4 mmol) was added to a solution of [(S)-3-hydroxy-7-methylazepan-4-ylcarbonyl]-3-methylbutyl]carbamic acid tert-butyl ester **53a, 53b** (1.0 g, 2.8 mmol) and *N*-methylmorpholine (0.45 mL, 4.1 mmol) in CH₂Cl₂ (35 mL) and was stirred at room temperature for 1 h. The reaction mixture was diluted with EtOAc (100 mL), washed with H₂O and brine, dried over magnesium sulfate, filtered, concentrated by rotary evaporation, and purified by column chromatography (silica gel, 2.5% MeOH/CH₂Cl₂) to yield the title compound as a mixture of diastereomers (0.9 g, 64%): ¹H NMR (CDCl₃) (as a mixture of two diastereomers): δ 8.71–8.68 (m, 1H), 8.08–7.92 (m, 2H), 7.57–7.49 (m, 1H), 6.76, 6.67 (brs each, 1H), 5.15–4.96 (m, 2H), 4.18–3.87 (m, 4H), 3.74–3.63 (m, 1H), 3.46–3.36 (m, 1H), 1.96–

assays were conducted at ambient temperature. Product fluorescence (excitation at 360 nm, emission at 460 nm) was monitored with a Perceptive Biosystems Cytofluor II fluorescent plate reader. Product progress curves were generated over 20–30 min following formation of AMC product.

Potential inhibitors were evaluated using the progress curve method. Assays were carried out in the presence of variable concentrations of test compound. Reactions were initiated by addition of enzyme to buffered solutions of inhibitor and substrate. Data analysis was conducted according to one of two procedures, depending on the appearance of the progress curves in the presence of inhibitors. For those compounds whose progress curves were linear, apparent inhibition constants ($K_{i,app}$) were calculated according to eq 1¹⁶

$$v = V_m A / [K_a (1 + I/K_{i,app}) + A] \quad (1)$$

where v is the velocity of the reaction with maximal velocity V_m , A is the concentration of substrate with Michaelis constant of K_a , and I is the concentration of inhibitor.

For those compounds whose progress curves showed the downward curvature characteristic of time-dependent inhibition, the data from individual sets was analyzed to give k_{obs} according to eq 2

$$[AMC] = v_{ss} t + (v_0 - v_{ss}) [1 - \exp(-k_{obs} t)] / k_{obs} \quad (2)$$

where $[AMC]$ is the concentration of product formed over time t , v_0 is the initial reaction velocity and v_{ss} is the final steady-state rate. Values for k_{obs} were then analyzed as a linear function of inhibitor concentration to generate an apparent second-order rate constant ($k_{obs}/\text{inhibitor concentration}$ or $k_{obs}/[I]$) describing the time-dependent inhibition. This kinetic treatment has been fully described.¹⁷

HPLC Method for Epimerization Study. The rates of C-4 epimerization were determined by HPLC analysis. The chromatographic conditions (1) for **2**, **4**, **11**, and **13** were as follows: column, XTerra RP18, 3.5 μm , 2.1 \times 100 mm (Waters Corp., Milford, MA); elution, isocratic with 47% A (acetonitrile), 53% B (20mM pH 7.4 phosphate); flow rate, 0.48 mL/min. The chromatographic conditions (2) for **1** (and **epi-1**) were as follows: column, Inertsil ODS3, 5 μm , 4.6 \times 250 mm (MetaChem Technologies Inc, Torrance, CA); elution, 50% A and 50% B; flow rate, 1 mL/min. An Agilent Model 1100 HPLC system with a diode array detector and ChemStation software was used for chromatographic data acquisition and processing. A 10 μL portion of DMSO stock solution containing the compound of interest (10 mM) was added into 1 mL of pH 11 phosphate buffer. The solution was quickly transferred to a HPLC sample vial and placed in the HPLC autosampler. Aliquots of the solution were injected immediately and subsequently at designated time intervals, and the chromatographic data were exported into an EXCEL table. The first-order forward rate constant, k , for the disappearance of the starting epimer can be determined on the basis of the following equation:

$$C(t)/C(0) = [R/(1 + R)] e^{-kt/(R+1)} + [1/(1 + R)]$$

$C(0)$ and $C(t)$ are concentrations at time = 0 and elapsed time t . R is the equilibrium ratio of product to reactant, calculated on the basis of HPLC peak areas for the epimer pairs at a long elapsed time.

NAMFIS and Conformational Analysis. Conformers for **1**, **2**, **7**, and **10** were generated by carrying out a 10 000-step Monte Carlo search in MacroModel 7.1¹⁸ using the MMFFs force field and chloroform implicit solvent model with an 8 kcal/mol cutoff. NOE and coupling constant information were obtained for protons at the chiral centers, amide nitrogens, pyridinyl group, and positions C2, C4, C5, C6, and C7. The NAMFIS algorithm was applied, and a best solution of conformers for each molecule was obtained. All NMR experiments for conformational analysis (**1**, **2**, **7**, and **10**) were performed on a Varian Inova 500 MHz spectrometer equipped with a 5 mm inverse detection probe with actively shielded

z -gradient at 25 °C. Samples were dissolved in CDCl_3 (99.96% deuterium) with an approximated concentration of 10 mM for each sample. ^1H NMR assignments were achieved according to conventional 1D proton and 2D gradient COSY and gradient HSQC experiments. Gradient COSY was collected with 16 scans, 2K data points (t_2) and 128 increments (t_1) with a spectral width of 4997.5 Hz in both dimensions. For gradient HSQC experiments, 128 t_1 increments of 2048 complex points with 16 scans each with a spectral width of 4997.5 Hz in F_2 and 20105.6 Hz in F_1 dimension were acquired. 2D NOESY spectra were collected with 32 scans, 2K data points (t_2) and 200 increments (t_1) with a spectral width of 4997.5 Hz in both dimensions, at mixing times of 50, 150, 200, 350, 500, 600, and 700 ms. NOE buildup curves were found to be linear within the tested mixing times (up to 700 ms). Interproton distances were derived on the basis of the NOE measurements from the NOESY spectra acquired with a mixing time of 500 ms for all four compounds. J coupling constants were measured from the proton spectra. In addition to the conformational searches carried out for azepanones **1**, **2**, **7**, and **10**, searches were also carried out for azepanone **3** as well as the thiol-adducts of azepanones **1**, **2**, **3**, **7**, and **10**, with methylmercaptan bonded to the original azepanone carbonyl carbon, resulting in an sp^3 -hybridized carbon center with a hydroxyl group (thiohemiketal) attached with the stereochemistry observed in the cathepsin K/azepanone cocrystal structures.

Crystallization and Structure Solution of the Complex of Cathepsin K with the Inhibitor 10. Crystals of mature activated cathepsin K at a concentration of 14 mg/mL in complex with **10** were grown at 10 °C by the vapor diffusion method in sitting drops from a solution of 28% PEG 400, 0.1 M Hepes buffer at pH 7.5 containing 0.2 M CaCl_2 . Crystals of the complex are hexagonal, space group $P6122$, with cell constants of $a = 74.84 \text{ \AA}$ and $c = 339.56 \text{ \AA}$. There are two protein–**10** complexes in the asymmetric unit. The crystal was flash-frozen in a nitrogen cold stream at $-180 \text{ }^\circ\text{C}$ for the data collection. The diffraction data were measured at beamline 17-ID in the facilities of the Industrial Macromolecular Crystallography Association Collaborative Access Team (IMCA-CAT) at the Advanced Photon Source. These facilities were established by the companies of the Industrial Macromolecular Crystallography Association through a contract with Illinois Institute of Technology (IIT), executed through IIT's Center for Synchrotron Radiation Research and Instrumentation. The structure was determined by molecular replacement with a model consisting of all protein atoms from the previously determined cathepsin K/E-64 complex (PDB ID 1ATK).⁹ The structure was refined at 2.5- \AA resolution with R_c of 0.24 and R_{free} of 0.28.

Pharmacokinetic Study Protocols. In vivo rat and monkey pharmacokinetic experiments were conducted as iv \times po crossover studies using $N = 3$ rats or monkeys per study using standard techniques. All studies were reviewed and approved by the GSK IACUC prior to initiation. Briefly, male Sprague–Dawley rats received the test compounds as a 1–2 mg/kg 0.5-h intravenous infusion via an indwelling femoral vein catheter; the same rats received a 2–4 mg/kg oral bolus gavage of the same compound 2 days later. Male cynomolgus monkeys received the test compounds as a 1–2 mg/kg 1-h intravenous infusion via a temporary saphenous vein catheter; the same monkeys received a 2–4 mg/kg oral bolus gavage of the same compound 7 days later. All dosages were administered as aqueous solutions containing <2% DMSO and <20% hydroxypropyl- β -cyclodextrin. Blood samples were obtained from a lateral tail vein (rats) or a femoral vein (monkeys) at timed intervals after each dosage and were centrifuged to obtain 50- μL plasma aliquots. LC/MS/MS was used to quantify drug concentrations in each sample, with a lower limit of quantitation that ranged from 1.0 to 10 ng/mL. Standard noncompartmental techniques were used to calculate pharmacokinetic parameters from the resulting concentration versus time data.¹⁹ In vitro plasma protein binding experiments were conducted using either equilibrium dialysis or ultrafiltration, according to standard techniques.²⁰

Madin–Darby Canine Kidney Cell Permeability. The in vitro cell permeability of selected compounds was determined using Madin–Darby canine kidney (MDCK, American Type Culture

Collection) cells. MDCK cells were maintained in modified Eagle's medium (MEM) containing 10% fetal bovine serum in an atmosphere of 5% CO₂ and 95% relative humidity at 37 °C. Cells were passaged at 80–90% confluence (every 3–4 days) using trypsin–EDTA solution (0.05% trypsin + 0.53 mM EDTA). MDCK cells were used between passage numbers 60–80. All cell culture reagents were purchased from either Sigma or Invitrogen Corp.

For the transport assay, cells were seeded on 12-well Transwells (0.4 μm polycarbonate filters, Corning Costar Corp.) at 100 000 cells per well. Cells were fed 24 h after seeding, and the assay was performed 48 h later. Immediately prior to the experiment, cell medium was removed and replaced with transport buffer (Hank's balanced salt solution (HBSS) containing 25 mM glucose and 25 mM *N*-(2-hydroxyethyl)piperazine-*N*-(2-ethanesulfonic acid, HEPES). Monolayers were allowed to equilibrate for approximately 1 h. The transport buffer was then removed and a dosing solution containing compound at a concentration of 10 μM in transport buffer was added to the apical (A) side of the monolayer. Blank transport buffer was added to basolateral (B) side of monolayer. DMSO was used as the initial solvent for compound dissolution, and then was diluted with transport buffer. The final DMSO concentration was 1% (v/v) in all dose solutions. Each treatment was done in duplicate. Propranolol and mannitol were included as controls.

After 1 h, aliquots of solutions in the donor and receiver compartments were diluted with acetonitrile and analyzed by LC/MS/MS. HPLC was accomplished using a Phenomenex Synergi Hydro-RP 4 μm, 2.1 × 50 mm column and a mobile phase consisting of 10 mM ammonium acetate (pH 6.8) and methanol. Compound product ion was generated using a Sciex API300 in turboionspray mode. Concentrations of each compound in apical and basolateral samples were determined from a peak area versus concentration standard curve. Standards were prepared from serial dilution of the initial dosing solution.

An apparent permeability coefficient (P_{app}) was calculated from the LC/MS/MS-determined concentration in the basolateral compartment (C_{BL}) and the nominal 10 μM concentration in the donor compartment, according to the equation below (units = nm/s), where 3600 s is the total time for the measurement of compound flux and 1.13 cm² is the area of the Transwell filter.

$$P_{app} = (C_{BL} \times 1.5 \text{ mL}) / 3600 \text{ s} / 1.13 \text{ cm}^2 / 10 \mu\text{M}$$

The coordinates for the complex of cathepsin K and **10** have been deposited in the Protein Data Bank, accession number 2FTD.

Acknowledgment. The authors would like to acknowledge Wanda Bodnar, Jo Salisbury, and Tim Tippin for conducting the MDCK permeability experiments.

Supporting Information Available: ORTEPs, crystal data, and coordinates for compounds **3**, **5**, **6**, **10**, **46**, and **47**. This material is available free of charge via the Internet at <http://pubs.acs.org>.

References

- Stroup, G. B.; Lark, M. W.; Veber, D. F.; Bhattacharyya, A.; Blake, S.; Dare, L. C.; Erhard, K. F.; Hoffman, S. J.; James, I. E.; Marquis, R. W.; Ru, Y.; Vasko-Moser, J. A.; Smith, B. R.; Tomaszek, T.; Gowen, M. Potent and Selective Inhibition of Human Cathepsin K Leads to Inhibition of Bone Resorption In Vivo in a Nonhuman Primate. *J. Bone Miner. Res.* **2001**, *16* (10), 1739–1746; Yamashita, D. S.; Dodds, R. A. Cathepsin K and the Design of Inhibitors of Cathepsin K. *Curr. Pharm. Des.* **2000**, *6* (1), 1–24; Marquis, R. W. Inhibition of the Cysteine Protease Cathepsin K. *Annu. Rev. Med. Chem.* **2004**, *39*, 79–98.
- Yamashita, D. S.; Smith, W. W.; Zhao, B.; Janson, C. A.; Tomaszek, T. A.; Bossard, M. J.; Levy, M. A.; Oh, H.-J.; Carr, T. J.; Thompson, S. K.; Ijames, C. F.; Carr, S. A.; McQueney, M.; D'Alessio, K. J.; Amegadzie, B. Y.; Hanning, C. R.; Abdel-Meguid, S.; DesJarlais, R. L.; Gleason, J. G.; Veber, D. F. Structure and Design of Potent and Selective Cathepsin K Inhibitors. *J. Am. Chem. Soc.* **1997**, *119* (46), 11351–11352; Marquis, R. W.; Yamashita, D. S.; Ru, Y.; LoCastro, S. M.; Oh, H.-J.; Erhard, K. F.; DesJarlais, R. L.; Head, M. S.; Smith, W. W.; Zhao, B.; Janson, C. A.; Abdel-Meguid, S. S.; Tomaszek, T. A.; Levy, M. A.; Veber, D. F. Conformationally Constrained 1,3-Diamino Ketones: A Series of Potent Inhibitors of the Cysteine Protease Cathepsin K. *J. Med. Chem.* **1998**, *41* (19), 3563–3567.
- Marquis, R. W.; Ru, Y.; LoCastro, S. M.; Zeng, J.; Yamashita, D. S.; Oh, H.-J.; Erhard, K. F.; Davis, L. D.; Tomaszek, T. A.; Tew, D.; Salyers, K.; Proksch, J.; Ward, K.; Smith, B.; Levy, M.; Cummings, M. D.; Haltiwanger, R. C.; Trescher, G.; Wang, B.; Hemling, M. E.; Quinn, C. J.; Cheng, H.-Y.; Lin, F.; Smith, W. W.; Janson, C. A.; Zhao, B.; McQueney, M. S.; D'Alessio, K.; Lee, C.-P.; Marzulli, A.; Dodds, R. A.; Blake, S.; Hwang, S.-M.; James, I. E.; Gress, C. J.; Bradley, B. R.; Lark, M. W.; Gowen, M.; Veber, D. F. Azepanone-Based Inhibitors of Human and Rat Cathepsin K. *J. Med. Chem.* **2001**, *44*, 1380–1395.
- Luzzio, F. A. The Henry Reaction: Recent Examples. *Tetrahedron* **2001**, *57*, 915–945.
- Grubbs, R. H. Olefin Metathesis. *Tetrahedron* **2004**, *60*, 7117–7140.
- Hendrickson, J. B. Molecular Geometry. V. Evaluation of Functions and Conformations of Medium Rings. *J. Am. Chem. Soc.* **1967**, *89*, 7036–7043. Favini, G. Conformational Analysis of Seven-Membered Cyclic Systems. *J. Mol. Struct.* **1983**, *93*, 139–152.
- Gula, M. J.; Vitale, D. E.; Dostal, J. M.; Trometer, J. D.; Spencer, T. A. Evaluation of 1,3-Diaxial Steric Hindrance to Proton Abstraction Alpha to Carbonyl Groups. *J. Am. Chem. Soc.* **1988**, *110*, 4400–4405.
- Nevins, N.; Cicero, D.; Snyder, J. P. A Test of the Single-Conformation Hypothesis in the Analysis of NMR Data for Small Polar Molecules: A Force Field Comparison. *J. Org. Chem.* **1999**, *64* (11), 3979–3986; Snyder, J. P.; Nevins, N.; Cicero, D. O.; Jansen, J. The Conformations of Taxol in Chloroform. *J. Am. Chem. Soc.* **2000**, *122* (4), 724–725.
- Zhao, B.; Janson, C. A.; Amegadzie, B. Y.; D'Alessio, K.; Griffin, C.; Hanning, C. R.; Jones, C.; Kurdyla, J.; McQueney, M.; Qui, X.; Smith, W. W.; Abdel-Meguid, S. S. Crystal Structure of Human Osteoclast Cathepsin K Complex with E-64. *Nat. Struct. Biol.* **1997**, *4* (2), 109–111.
- James, I. E.; Lark, M. W.; Zembryki, D.; Lee-Ryckaczewski, E. V.; Hwang, S. M.; Tomaszek, T. A.; Belfiore, P.; Gowen, M. Development and Characterization of a Human in Vitro Resorption Assay: Demonstration of Utility Using Novel Antiresorptive Agents. *J. Bone Miner. Res.* **1999**, *14*, 1562–1569.
- Thompson, M.; Lennox, R. B.; McClelland, R. A. Structure and Electrochemical Properties of Microfiltration Filter-lipid Membrane Systems. *Anal. Chem.* **1982**, *54*, 76–81; Kansy, M.; Senner, F.; Gubernator, K. Physicochemical High Throughput Screening: Parallel Artificial Membrane Permeation Assay in the Description of Passive Absorption Processes. *J. Med. Chem.* **1998**, *41*, 1007–1010.
- Turk, D.; Podobnik, M.; Popovic, T.; Katunuma, N.; Bode, W.; Huber, R.; Turk, V. Crystal Structure of Cathepsin B Inhibited with CA030 at 2.0-Å Resolution: A Basis for the Design of Specific Epoxysuccinyl Inhibitors. *Biochemistry* **1995**, *34*, 4791–4797.
- Veber, D. F.; Johnson, S. R.; Cheng, H.-Y.; Smith, B. R.; Ward, K. W.; Kopple, K. D. Molecular Properties That Influence the Oral Bioavailability of Drug Candidates. *J. Med. Chem.* **2002**, *45*, 2615–2623.
- Lipinski, C. A.; Lombardo, F.; Dominy, B. W.; Feeney, P. J. Experimental and Computational Approaches To Estimate Solubility and Permeability in Drug Discovery and Development Settings. *Adv. Drug. Del. Rev.* **2001**, *46*, 3–26.
- Ertl, P.; Rohde, B.; Selzer, P. Fast Calculation of Molecular Polar Surface Area as a Sum of Fragment-Based Contributions and Its Application to the Prediction of Drug Transport Properties. *J. Med. Chem.* **2000**, *43*, 3714–3717.
- Brandt, M.; Levy, M. A. 3β-Hydroxy-Δ⁵-steroid Dehydrogenase/3-Keto-Δ⁵-steroid Isomerase from Bovine Adrenals: Mechanism of Inhibition by 3-Oxo-4-aza Steroids and Kinetic Mechanism of the Dehydrogenase. *Biochemistry* **1989**, *28*, 140–148.
- Morrison, J. F.; Walsh, C. T. The Behavior and Significance of Slow-Binding Enzyme Inhibitors. *Adv. Enzymol. Relat. Areas Mol. Biol.* **1988**, *61*, 201–301.
- Mohamadi, F.; Richards, N. G. J.; Guida, W. C.; Liskamp, R.; Lipton, M.; Caufield, C.; Chang, G.; Hendrickson, T.; Still, W. C. MacroModel—An Integrated Software System for Modeling Organic and Bioorganic Molecules Using Molecular Mechanics. *J. Comput. Chem.* **1990**, *11* (4), 440–467.
- Gabrielsson, J.; Weiner, D. *Pharmacokinetic and Pharmacodynamic Data Analysis: Concepts and Applications*; Apotekarsocieteten: Stockholm, 1997.
- Pacifici, G. M.; Viani, A. Methods of Determining Plasma and Tissue Binding of Drugs. Pharmacokinetic Consequences. *Clin. Pharmacokinetic.* **1992**, *23*, 449–468.